

Original Article

Cite this article: Garza HK, Catlos EJ, Brookfield ME, Malkowski MA, Chamberlain KR, Loewy SL, and Stockli DF. Detrital U-Pb ages for the first well-preserved vascular plant *Cooksonia* from the UK and Irish macrofossil record. *Geological Magazine* 161(e19): 1–15. <https://doi.org/10.1017/S0016756824000384>

Received: 22 March 2024
Revised: 11 August 2024
Accepted: 20 September 2024




Keywords:

Geochronology; Paleobotany; LA-ICP-MS; U-Pb; *Cooksonia*; Silurian; Biostratigraphy

Corresponding author:

Hector K Garza;
Email: hector.garza@utexas.edu

Detrital U-Pb ages for the first well-preserved vascular plant *Cooksonia* from the UK and Irish macrofossil record.

Hector K Garza^{1,2} , Elizabeth J Catlos^{1,2} , Michael E Brookfield¹ ,
Matthew A Malkowski¹, Kevin R Chamberlain³, Staci L Loewy¹ and Daniel F Stockli¹

¹Department of Earth and Planetary Sciences, University of Texas at Austin, Austin, TX, USA; ²Center for Planetary Systems Habitability, University of Texas at Austin, Austin, TX, USA and ³Department of Geology and Geophysics, University of Wyoming, Laramie, WY, USA

Abstract

The emergence of vascular plants, such as *Cooksonia*, had a profound impact on Earth's Early Paleozoic biogeochemical cycles (e.g. atmospheric oxygen, nitrogen and CO₂), potentially triggering global environmental and biological changes. However, the timing of *Cooksonia*'s terrestrial emergence remains elusive as phylogenetic models, microfossils and macrofossils provide different timings for land colonization by vascular plants. Here, hundreds of zircon grains from three siltstones were dated using Laser Ablation-Inductively Couple Plasma-Mass Spectrometry (LA-ICP-MS). The study presents detrital **zircon U-Pb** dates, which refine the current biostratigraphy ages assigned to *Cooksonia* macrofossils from the three oldest sites globally. Specifically, siltstones hosting *Cooksonia* macrofossils from Borrishnoe Mountain (Ireland) and Capel Horeb (Wales) yield Gorstian–Homerian maximum depositional ages (MDAs) of 426 ± 2 Ma and 427 ± 2 Ma, respectively. Additionally, Cwm Graig Ddu (Wales) yields a (Pridoli-Ludlow) maximum age of 423 ± 3 Ma. The findings provide the first detrital **zircon U-Pb** dates for the oldest *Cooksonia* macrofossils globally and contribute crucial maximum ages. These maximum ages are instrumental in refining future calibrations of molecular clocks and improving phylogenetic models, thus contributing significantly to a better understanding of *Cooksonia*'s evolutionary history, including its environmental and ecological impacts.

1. Introduction

The transition of plants from water to land took hundreds of millions of years, with numerous progressive innovations and adaptations, reshaping Earth's terrestrial landscapes in profound ways (Kenrick *et al.*, 2012; De Vries & Archibald, 2018). Macrofossils, spores and phylogenetic models **provide various answers as to when vascular plants colonized land, contributing to a multitude of hypotheses** (Kenrick *et al.*, 2012; Edwards *et al.*, 2014; Edwards & Kenrick, 2015; Salamon *et al.*, 2018). While molecular phylogenies suggest that vascular plants originated in the Middle Cambrian period (~500 Ma) (Morris *et al.*, 2018; Servais *et al.*, 2019; Donoghue *et al.*, 2021), the presence of spores attributed to non-vascular land plants, known as cryptospores, is documented only from Middle Ordovician (Darrivilian stage; 468–461 Ma) sediments onwards (Stemans *et al.*, 2009; Morris *et al.*, 2012; Edwards & Kenrick, 2015). Additionally, tetrad spores, widely considered to originate from vascular plants, emerged during the Late Ordovician (Katian stage; ~450 Ma) (Fig. 1a; Table 1) (Strother *et al.*, 1996; Wellman & Gray, 2000; Stemans *et al.*, 2009; Edwards and Kenrick, 2015). Macrofossils of vascular plants, exemplified by *Cooksonia*, appear only in the mid- to late Silurian (Wenlockian stage ~ 430 Ma onwards), though fragmentary remains seem to appear earlier in the mid- to late Ordovician (Fig. 1a; 1b; Table 1) (Wellman *et al.*, 2003; Xu *et al.*, 2022).

One challenge arises from the lack of close modern analogues for cryptospores, except for a few spore configurations found in select liverworts (Renzaglia *et al.*, 2015a, b). Cryptospores exhibit a sudden decline in taxonomic diversity and abundance during the Early Devonian period (latest Lochkovian, ~410 Ma), with only a few forms persisting through to the late Early Devonian (Emsian stage; 408–393 Ma) (Wellman *et al.*, 2013). Another complication concerns the preservation of diagnostic features of vascular plants, such as conducting tissue. The earliest preserved fragments displaying stomata-bearing epidermis, trilete spores and well-developed tracheids with distinct lateral wall facets, but without sporangia, date back to the lower Sandbian period (Upper Ordovician, ~ 458 Ma) of Inner Mongolia (Xu *et al.*, 2022). However, there is then a gap until these features are recorded, with sporangia first appearing in the Wenlockian period (~430 Ma) in Europe (Edwards & Davis, 1976).

© The Author(s), 2024. Published by Cambridge University Press. This is an Open Access article, distributed under the terms of the Creative Commons Attribution licence (<https://creativecommons.org/licenses/by/4.0/>), which permits unrestricted re-use, distribution and reproduction, provided the original article is properly cited.

Table 1. Micro- and macrofossil compilation of vascular plants from previous studies estimating the fossil age from biostratigraphy

Locality	Fossil	Biostratigraphy for age	Age/stage	References
Saudi Arabia	Trilete spores	Acritarchs, Chitinozoans	Late Ordovician/Katian	1
Poland	Polysporangiophyte	Acritarchs, Chitinozoans	Late Ordovician/Hirnantian	2
Ireland	Cooksonia	Graptolites	Middle Silurian/Homerian	3,4
Wales	Cooksonia	Graptolites	Late Silurian/Gorstian	5
Wales	Cooksonia	Acritarchs, Invertebrates	Late Silurian/Ludfordian	6,7

References 1. Strother *et al.* (1996); 2. Salomon *et al.* (2018); 3. Edwards & Feehan, (1980); 4. Edwards *et al.* (1983); 5. Edwards *et al.* (1979); 6. Edwards & Davies, (1976); 7. Edwards & Rogerson, (1979).

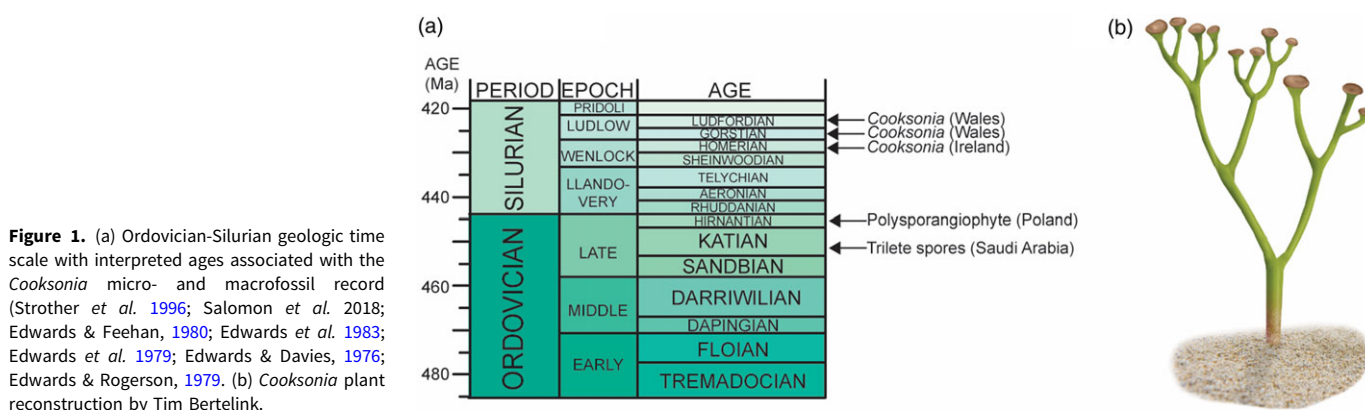


Figure 1. (a) Ordovician-Silurian geologic time scale with interpreted ages associated with the *Cooksonia* micro- and macrofossil record (Strother *et al.* 1996; Salomon *et al.* 2018; Edwards & Feehan, 1980; Edwards *et al.* 1983; Edwards *et al.* 1979; Edwards & Davies, 1976; Edwards & Rogerson, 1979). (b) *Cooksonia* plant reconstruction by Tim Bertelink.

In the Early Paleozoic, the development of primitive root hair structures by *Cooksonia* wielded a transformative influence on Earth. This transformation was manifested by amplified weathering rates, soil development, landscape stabilization and consequential alterations to Earth's biogeochemical cycles, encompassing atmospheric oxygenation, and the carbon and nitrogen cycles (Wellman, 2010; Lenton *et al.*, 2012; Salomon *et al.*, 2018; Yuan *et al.*, 2023). These alterations reverberated across climate systems and terrestrial ecosystems with some studies associating early lands plants as a potential catalyst of the Late Ordovician Mass Extinction (LOME) and the facilitators for the transition of arthropods from aquatic to terrestrial environments (Garwood & Edgecombe, 2011; Kenrick *et al.*, 2012; Dunlop *et al.*, 2013; Lenton *et al.*, 2016; Wallace *et al.*, 2017; Dahl & Arens, 2020). Additionally, previous studies linking the colonization of land plants to the Hirnantian glaciation – triggering the onset of LOME – demonstrates the necessity for more precise dating of terrestrial plants during the Ordovician period to refine the accuracy of phylogenetic trees, biogeochemical cycles and extinction models (Lenton *et al.*, 2012). The actual time at which these first vascular plant fossils appeared is often hard to determine, because it is difficult to correlate biostratigraphy from lake, river and coastal environment deposits in which they occur, with the standard marine-based geological time scale (Finney & Chen, 1990; Pogson, 2009; Brookfield *et al.*, 2021). Hence, a robust U-Pb dating approach becomes imperative.

In this study, we present comprehensive data encompassing mineralogical X-ray diffraction (XRD), X-ray fluorescence (XRF) and the first detrital zircon U-Pb Laser Ablation-Inductively Coupled Plasma-Mass Spectrometry (LA-ICP-MS) dates from the three oldest sites (Middle to Late Silurian) containing *Cooksonia* macrofossils. These notable locations are situated in Ireland

(Borrisnoe Mountain) and Wales (Capel Horeb and Cwm Graig Ddu, United Kingdom) (Fig. 2). We employ the well-established 'Law of Detrital Zircon' – a sedimentary rock is age-equivalent or younger than its youngest constituent zircon grains to establish maximum depositional ages (MDAs) for the siltstones bearing *Cooksonia* macrofossils within these localities, previously dated solely via biostratigraphy. These dates refine the timing of the earliest well-preserved vascular plant *Cooksonia* macrofossils.

2. Geological setting

2. a. Capel Horeb Quarry, Powys, Wales, UK

Capel Horeb Quarry in Powys, Wales, is the third-oldest known site harbouring *Cooksonia*'s macrofossils within the Upper Roman Camp Formation (Figs. 1a & 3; Table 1) (Specimen-NMW 69.64G, National Museum of Wales) (Cleal & Thomas, 1995; Edwards & Richardson, 2004). The Silurian stratigraphic section at this location was initially interpreted as Ludlovian by Potter & Price (1965). Their description includes mudstone, shale, siltstone and sandstone. The stratigraphic sequence begins with the Black Cock Beds, estimated to be 870 ft.-thick, comprising silty mudstone, flaggy mudstone and siltstone and containing abundant marine fauna fossils. Subsequently, the Black Cock Beds are succeeded by the ~810 ft.-thick Cwm Clyd Beds, which are characterized by siltstone, flaggy shaly sandstone and silty mudstone with a profusion of marine fauna fossils. Overlying the Cwm Clyd Beds are the Roman Camp Beds, further divided into the Lower Roman Camp Beds (360 ft. thick) and the Upper Roman Camp Beds (310 ft. thick). The Lower Roman Camp Beds are primarily composed of shaly siltstone, grey flaggy siltstone and sandstone, all

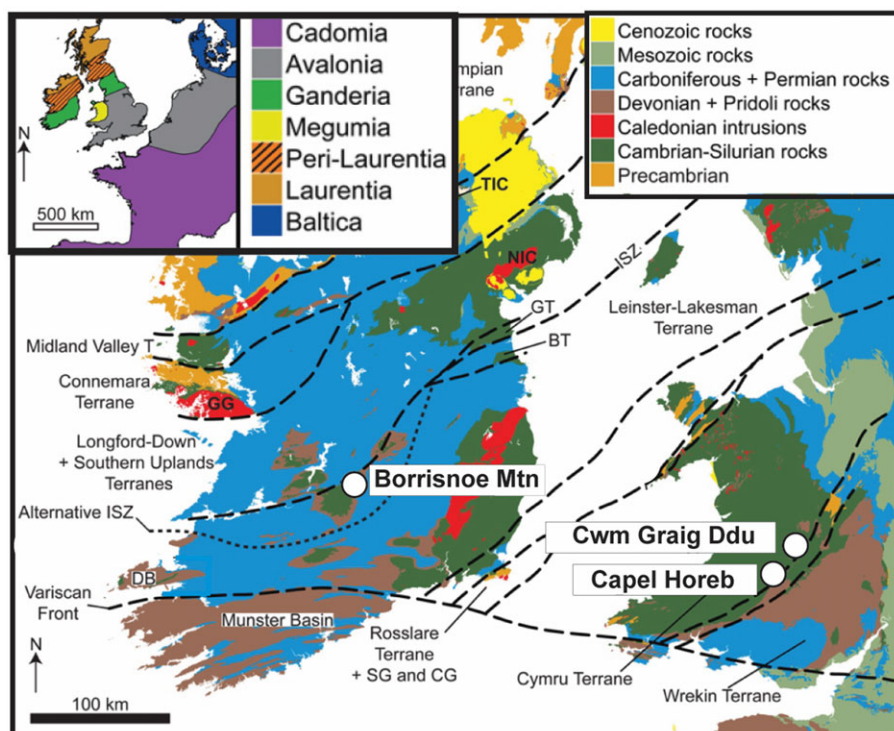


Figure 2. Generalized terrane map of the UK and Ireland showing localities hosting *Cooksonia*'s earliest macrofossils (after Fairley *et al.*, 2018).

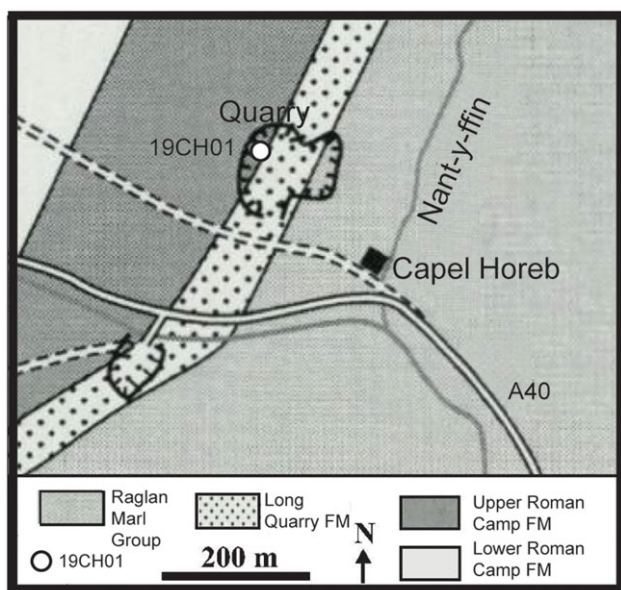


Figure 3. Capel Horeb geologic map showing location of quarry and sample 19CH01. Modified from Lane (2000).

bearing abundant marine fossils. In contrast, the Upper Roman Camp Beds are alternating grey and blue shaly siltstone and flaggy massive calcareous sandstone. Notably, Potter and Price (1965) observed a decrease in fossils within the Upper Roman Camp Beds but reported the presence of fossilized plant remains.

The plant remains were initially found by Heard (1939) in the Upper Roman Camp Beds, and Edwards and Davies (1976) described the *Cooksonia* macrofossils with an assigned Upper Ludlow (Ludfordian) age based on invertebrate and acritarchs biostratigraphy (Edwards and Rogerson, 1979; Edwards & Richardson, 2004). However, there have also been reports of

Pridoli age *Cooksonia* macrofossils in the sequence (Cleal & Thomas, 1995). The plant fragments are most abundant in the grey blue flaggy siltstone beds within the Upper Roman Camp Beds. Based on the biostratigraphy, the depositional environment has been interpreted as an inshore marine environment (Cleal & Thomas, 1995; Edwards & Richardson, 2004).

2. b. Cwm Graig Ddu, Powys, Wales, UK

The Cwm Graig Ddu Quarry in Powys, Wales, is the second oldest known location containing *Cooksonia*'s macrofossils (Figs. 1a & 4; Table 1). Straw (1952) characterized the Silurian stratigraphic sequence at Cwm Graig Ddu as a succession of Lower and Upper Ludlow age shale, mudstone and siltstone. The sequence begins with the 1150 ft.-thick Lower Main Slump Group mudstone, followed by the 350 ft.-thick Shales with Thin Slumps, and the 140 ft.-thick Upper Slump Group Shales. All these units are associated with the Lower Ludlow age graptolite *Monograptus scanicus*. The Upper Slump Group Shales are succeeded by the 1150 ft.-thick *Pterinea tenuistriata* shale beds, the 750 ft.-thick *Lingula lata* shale beds and the 300 ft.-thick *Chonetoida grayi* mudstone beds, attributed to the Lower Ludlow age *Monograptus tumescens* and *Monograptus leintwardinensis* graptolites. Straw (1952) documented marine fauna in the Lower Ludlow *Pterinea* beds, consisting of graptolites, crinoids, brachiopods, cephalopods, pelecypods, gastropods and plant fragment remains. The *Pterinea* beds are comprised of platy shale with its lower half exhibiting laminated shale and its upper half with interbedded shale with coarse lenticular siltstone (Straw, 1952). *Cooksonia* specimen-NMW 79.17G housed in the National Museum of Wales was located within the *Pterinea* Beds (Cleal & Thomas, 1995; Edwards & Richardson, 2004).

Cooksonia specimens from the *Pterinea* beds were described by Edwards *et al.* (1979) based on Straw's (1952) detailed account (Edwards & Richardson, 2004). The lithology and fossil content of the *Pterinea* beds and the surrounding area indicate a near shore

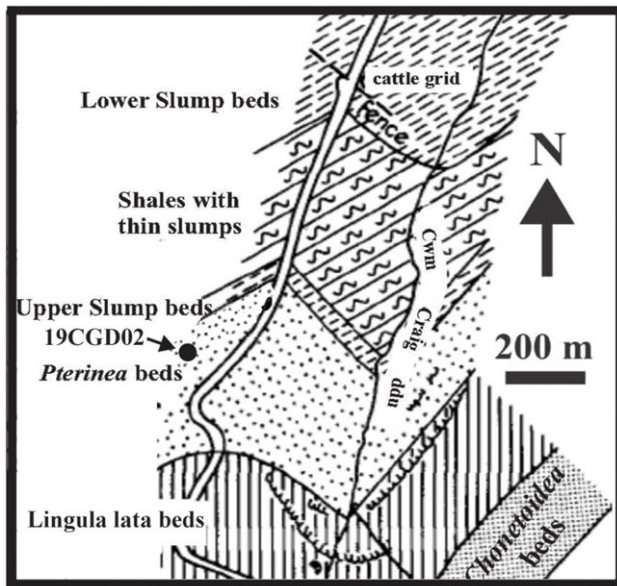


Figure 4. Cwm Graig Ddu geologic map showing location of sample 19CGD02. Modified from Straw (1952).

deltaic depositional environment (Cleal & Thomas, 1995). This setting is particularly suitable for understanding the transition of plants from marine to terrestrial environments (Edwards *et al.*, 1979). *Cooksonia* macrofossils were recovered from light grey micaceous flaggy siltstones and dark grey siltstones. The lithology in this area primarily consists of slumped fine-grained siltstones and sandstones, along with shales and mudstones. The presence of slumped beds within the *Pterinea* beds suggests a paleo-slope in the eastern Welsh basin, implying that the plant remains likely originated from the direction of the shelf and land (Edwards *et al.*, 1979).

Notably, the graptolite zones have been reevaluated since Straw's (1952) interpretations, with the original Ludlow *Monograptus tumescens* zone being revised to the assessed Ludlow Gorstian age *Monograptus incipiens* zone (Edwards *et al.*, 1979; Edwards & Richardson, 2004). It is worth mentioning that the currently established graptolite biozones have undergone a reassessment, leading to changes in nomenclature, including the removal of the *Monograptus tumescens* and *Monograptus incipiens* zones, and the renaming of *Monograptus leintwardinensis* to *Saetograptus leintwardinensis* (Melchin *et al.*, 2020).

2. c. Borrisnoe Mountain, County Tipperary, Ireland

Borrisnoe Mountain in County Tipperary, Ireland, hosts the oldest macrofossils of the *Cooksonia* genus in the Hollyford Formation (Figs. 1a & 5; Table 1) (Edwards & Feehan 1980; Edwards *et al.*, 1983; Edwards & Kenrick, 2015). Tectonism and fault systems in the area coupled with limited rock exposures led to considerable variations in stratigraphic and lithological descriptions of the region. Cope (1954, 1959) initially divided the area's stratigraphic sequences into two groups, the Lower Ludlow-age Cloncannon Formation defined by the *Monograptus tumescens* graptolite zone and the Upper Wenlock-age assemblage characterized by *Cyrtograptus lundgreni*. According to Cope's (1959) interpretation, both assemblages share similar lithologies, consisting of mudstone, siltstone and greywacke. Siltstone constitutes approximately half of the Cloncannon Formation's volume. Cope (1959) identified four types of siltstones facies, described as laminated, flaggy, graded-bed

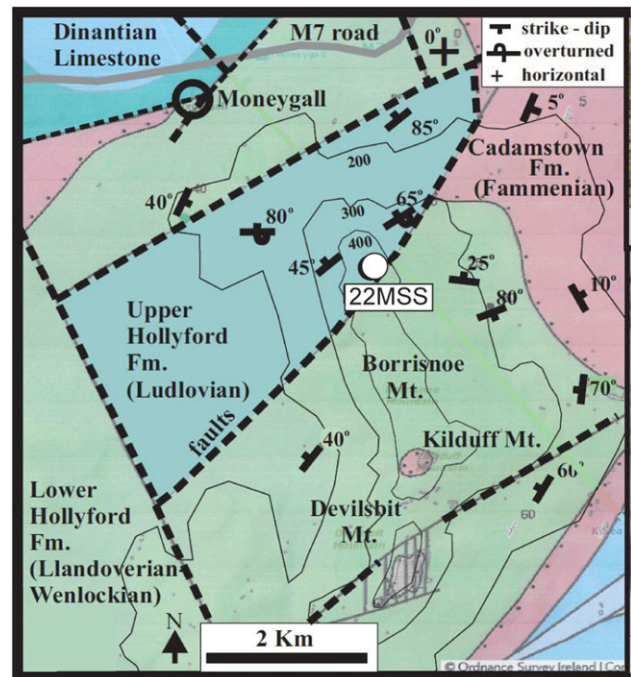


Figure 5. Geologic and tectonic map of Borrisnoe Mountain in County Tipperary, Ireland, with location of analysed sample 22MSS (modified from Irish Geological Survey solid map and Cope, 1959).

and micaceous. Plant remains were reported in the micaceous siltstones, suggesting a brackish water environment (Cope, 1959).

Doran (1974) and Archer (1981) recognized a single formation at Borrisnoe Mountain and termed it the Hollyford Formation. Cope's (1959) Cloncannon Formation occurs in an isolated fault-bounded block and is younger than the rest of the sediments, and we use the term upper Hollyford Formation for the Ludlow age sediments, and lower Hollyford Formation for the mass of Wenlock age sediments surrounding them. According to Doran (1974), the lithological composition of the Hollyford Formation consists of 60% greywacke, 25% mudstone and 15% laminated siltstone, indicating a marine environment associated with the Upper Wenlock age based on *Cyrtograptus lundgreni*. Archer (1981) described the Hollyford Formation as being characterized by extensive turbidite deposits comprising mudstone, sandstone and conglomerate, indicative of a marine fan environment.

Edwards and Feehan (1980) described and attributed the *Cooksonia* fossil (Specimen-TCD 22944, Geological Museum, Trinity College Dublin) from the micaceous siltstones to the Cloncannon Formation, which in this study will be attributed to the Hollyford Formation. The unit containing the plant fossils within the Hollyford Formation has been reassessed to the graptolite zone of *Monograptus ludensis*, placing it in the mid-Silurian (Late Wenlock ~ 427.4 – 430.5 Ma) (Edwards & Feehan, 1980). As described by Edwards *et al.* (1983), the depositional environment of the Hollyford Formation is a marine succession within a submarine fan, featuring turbiditic sandstones, conglomerates, mudstones, and laminated siltstones with sparse volcanic clasts (Edwards & Feehan, 1980; Edwards *et al.*, 1983).

3. Methods

This study involved the data acquisition of XRF, XRD and U-Pb detrital zircon dates from three siltstone samples (22MSS,

19CGD02, 19CH01), bearing the three earliest-recorded *Cooksonia* macrofossils found in sites across Wales and Ireland. Sample 22MSS is sourced from the Hollyford Formation, situated in Borrishnoe Mountain, County Tipperary, Ireland (52°51'15.82" N, 7°55'16.10" W), linked to specimen TCD 22944 from the Geological Museum at Trinity College, Dublin, Ireland (Edwards & Feehan, 1980; Edwards *et al.*, 1983). Sample 19CGD02 originates from the Pterinea Beds within Cwm Graig Ddu Quarry, Powys, Wales (52°6'49.50" N, 3°31'14.70" W), correlated with specimen NMW 79.17G from the National Museum of Wales (Edwards *et al.*, 1979; Cleal & Thomas, 1995; Edwards & Richardson, 2004). Sample 19CH01 is from the Upper Roman Camp Beds at Capel Horeb Quarry, Powys, Wales (51°58'40.98" N, 3°41'1.20" W), associated with specimen NMW 69.64G from the National Museum of Wales (Edwards & Rogerson, 1979; Edwards *et al.*, 1979; Edwards, 1982; Cleal & Thomas, 1995; Edwards & Richardson, 2004).

Traditional heavy mineral separation techniques were used following modified methods by Garza *et al.* (2023). All zircon grains were annealed for 50 hours at 850 °C to repair fission tracks, minor radiation damage, reduce isotopic fractionation and improve accuracy of LA-ICP-MS data (Mattinson, 2005; Allen & Campbell 2012). A total of 787 zircon grains were mounted on double-sided tape and inspected with backscatter electron (BSE) imaging using a JEOL Scanning Microscope at the University of Texas at Austin (UT Austin), GeoMaterials Characterization and Imaging facility (GeoMatCI). Following imaging, the zircon grains were dated using Element2 High Resolution (HR)-LA-ICP-MS in the Geo-Thermochronology Laboratory at UT Austin. The instrument uses an Eximer (192 nm) laser ablation system and obtains isotopic measurements using ion counting. A dry ablated aerosol is introduced to the instrument by pure He carrier gas containing the desired isotopic analytes, which for this study consists of ^{238}U , ^{235}U , ^{232}Th , ^{206}Pb , ^{207}Pb and ^{208}Pb . Each analysis consists of a 2-pulse cleaning ablation, a background measurement taken with the laser off, a 30-second measurement with the laser firing and a 30-second cleaning cycle. The laser beam was 20 μm in diameter to analyses grains as small as 50 μm . Elemental isotopic fractionation of Pb and Pb/U isotopes was corrected by interspersed analyses of primary and secondary zircon standards with known ages (GJ1 and Plesovice references) (Jackson *et al.*, 2004; Sláma *et al.*, 2008). The typical ratio of unknown standards measurements was 4:1 or 5:1. Systematic uncertainties resulting from calibration corrections are usually 1-2% for $^{206}\text{Pb}/^{207}\text{Pb}$ and $^{206}\text{Pb}/^{238}\text{U}$. Fully propagated errors utilized for U-Pb zircon dates. Pb values are reported as total Pb without any correction for potential common ^{204}Pb due to isobaric interferences with ^{204}Hg . Iolite 4 software was used to process and reduce data analyses, correct instrument drift and downhole fractionation (<https://iolite-software.com>).

Statistical values, MDAs and figures were produced by Isoplot/Ex, Densityplotter and detritalPy with a bandwidth of ten (Ludwig, 2008; Vermeesch, 2012; Sharman *et al.*, 2018). The LA-ICP-MS U-Pb dates underwent two interpretations. One approach involved applying a $^{206}\text{Pb}/^{238}\text{U}$ vs $^{207}\text{Pb}/^{235}\text{U}$ and $^{206}\text{Pb}/^{238}\text{U}$ vs $^{206}\text{Pb}/^{207}\text{Pb}$ 10% discordance filter across the entire dataset, reducing the number of dates from 787 to 378. Conversely, the other method entailed employing the ^{207}Pb method as the common Pb correction for the ^{238}U - ^{206}Pb dates up to 900 Ma for a total of 553 zircon dates. The ^{207}Pb correction method removes common Pb by utilizing the measured $^{207}\text{Pb}/^{206}\text{Pb}$ ratio to project any data point to concordia. This method assumes that the sample's radiogenic Pb component from the U-Pb data are concordant (Andersen, 2002; Chew *et al.*, 2011; White & Ireland, 2012; Chew *et al.*, 2014).

For the determination of the youngest single grain (YSG) MDA, calculations were based on the youngest zircon date derived from the 10% discordance filter dataset (Ludwig & Mundil, 2002). Meanwhile, the youngest cluster of 3+ grains ($\text{YC}2\sigma+3$) was determined by computing the weighted mean of the youngest zircon grain cluster consisting of three or more grains, which overlapped at 2σ uncertainty from the 10% discordance filter dataset (Dickinson & Gehrels, 2009). Moreover, the youngest mode weighted mean (YMWM) was calculated following the method outlined by Tian *et al.* (2022). This involved using LA-ICP-MS zircon dates that constituted the youngest age mode from a kernel density estimation (KDE) peak, calculating a weighted mean of more than three grains overlapping at 2σ uncertainty, with an approximate MSWD of 1 (Garza *et al.*, 2023). In this study, the YMWM was computed from ^{238}U - ^{206}Pb dates up to 900 Ma using two different approaches: with a 10% discordance filter, and with a common Pb correction. Additionally, the YMWM was determined with three different KDE bandwidths (8, 10 and 12), while maintaining a consistent bin size of 5.

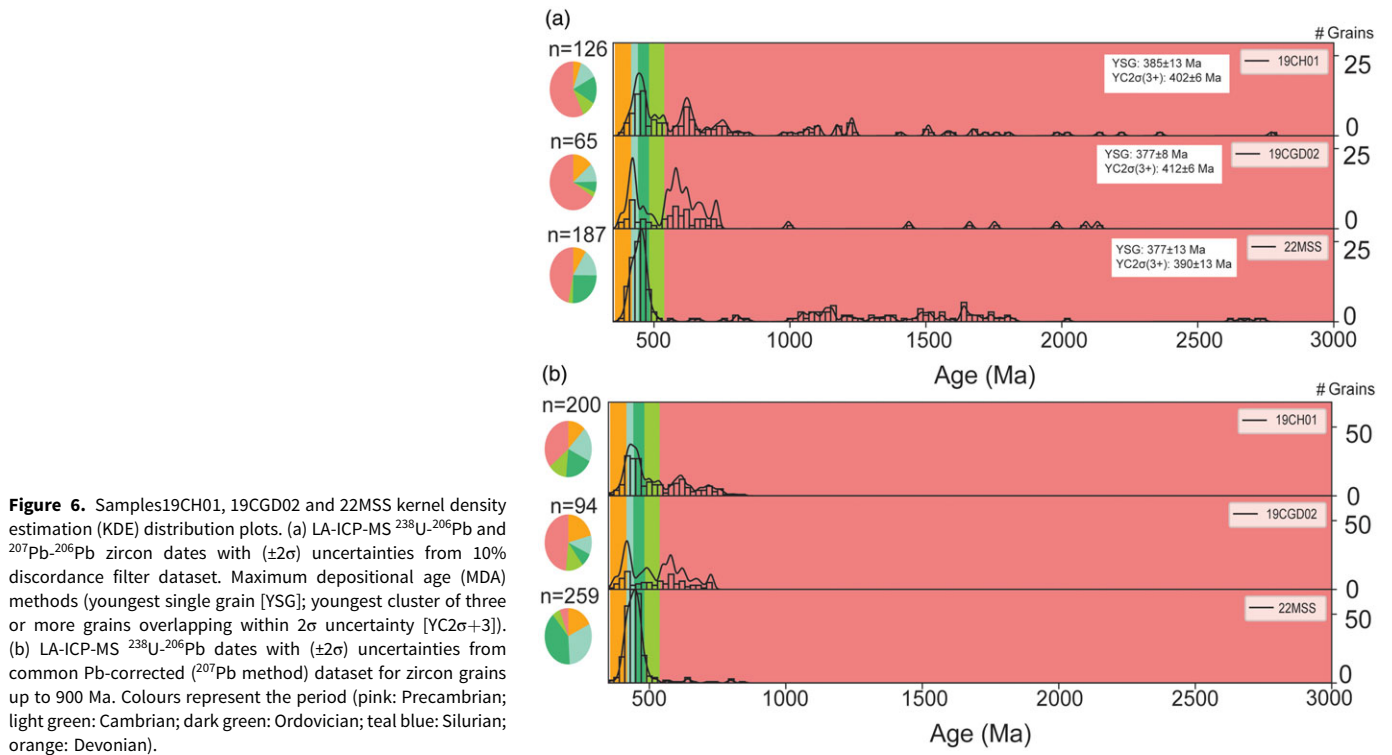
In addition to the zircon dates, whole rock mineralogical (XRD data) were obtained from all dated samples at the GeoMatCI facility at UT Austin. Whole rock samples were manually homogenized, ground and sieved to a 250 μm mesh size. XRD analyses were performed using a Bruker D8 instrument equipped with Cu K α radiation and a nickel filter, along with a LYNXEYE solid-state detector. The analyses were carried out at a voltage of 45 kV and a current of 40 mA, employing a 2θ scan axis ranging from 3° to 70°, with step increments of .0195° (2θ) and a duration of 1 s per step. Whole rock X-ray patterns were determined through Rietveld refinement utilizing Bruker TOPAS 4.2 software.

Whole rock elemental compositions were obtained using a portable XRF instrument at the University of Texas at Austin following the method of Rowe *et al.* (2012). Samples were grounded for homogenization, pressed into a pellet and analysed using a Bruker S1 Titan 800 ED-XRF (portable XRF) instrument equipped with Rh X-ray tube. Analyses consisted of 15 Kv excitation voltage for major elements for 30 seconds and 50 Kv excitation voltage for trace elements for 60 seconds. XRF analyses were calibrated modifying the Bruker MudRock Air calibration and generating our own clastic rock standards. Our references consist of five international commercially available accepted standards (SBC-1, SGR-1b, SCo-2, ShBOQ-1 and SRM 70b) and five siltstone/sandstone internal standards. Elemental tectonic setting discrimination diagrams for siliciclastic sediments plotted after Roser & Korsh (1986), Verma & Armstrong-Altrin (2013), Sahraeyan *et al.* (2015) and Rollinson & Pease (2021).

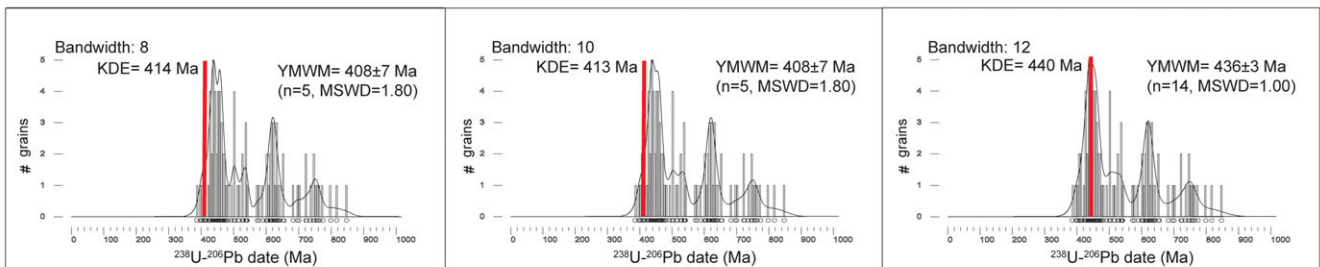
4. Results

4. a. Capel Horeb Quarry, Powys, Wales, UK

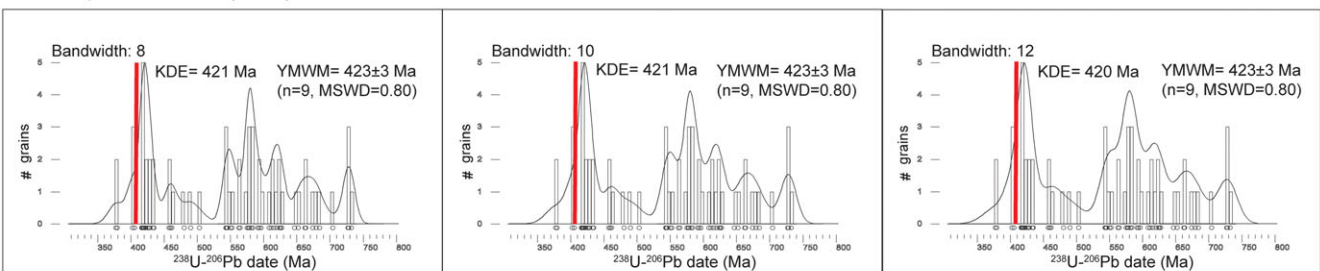
Sample 19CH01 obtained from the Upper Roman Camp Formation produced a total of 126 zircon dates post-application of a $\leq 10\%$ discordance filter. These dates span from the Precambrian to the Devonian and serve to determine an MDA for the blue flaggy siltstone beds within the Upper Roman Camp Formation (Fig. 6a; supplementary table S1). The youngest MDA estimate is the YSG date of 385 ± 13 Ma (10% disc), while the $\text{YC}2\sigma+3$ estimation presents a date of 402 ± 6 Ma ($n = 5$, MSWD = 1.80). The YMWM with various bandwidths provides dates of 408 ± 7 Ma ($n = 5$, MSWD = 1.80, bandwidth = 8), 408 ± 7 Ma ($n = 5$, MSWD = 1.80, bandwidth = 10) and 436 ± 3 Ma ($n = 14$, MSWD = 1.00, bandwidth = 12) (Fig. 7a).



(a) Sample 19CH01 (n=92)



(b) Sample 19CGD02 (n=58)



(c) Sample 22MSS (n=108)

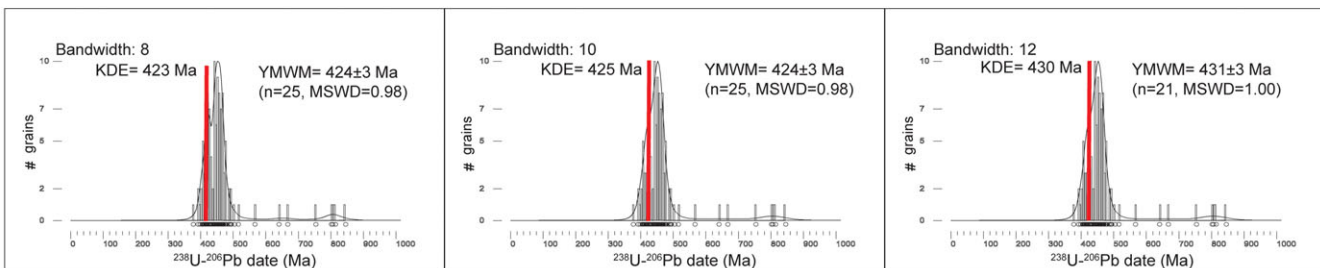
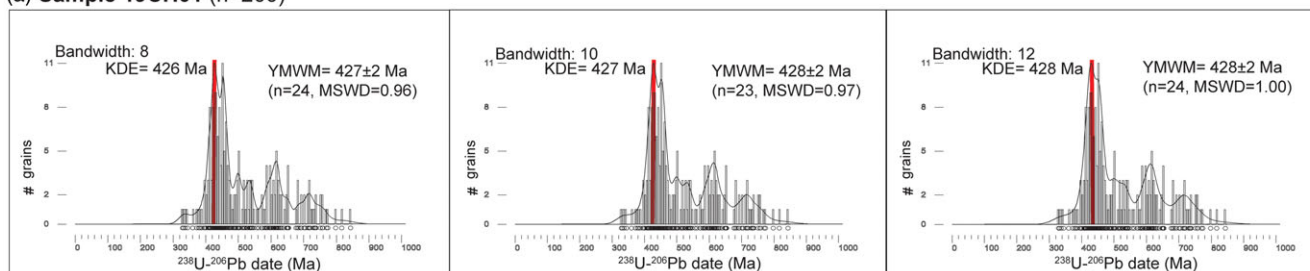
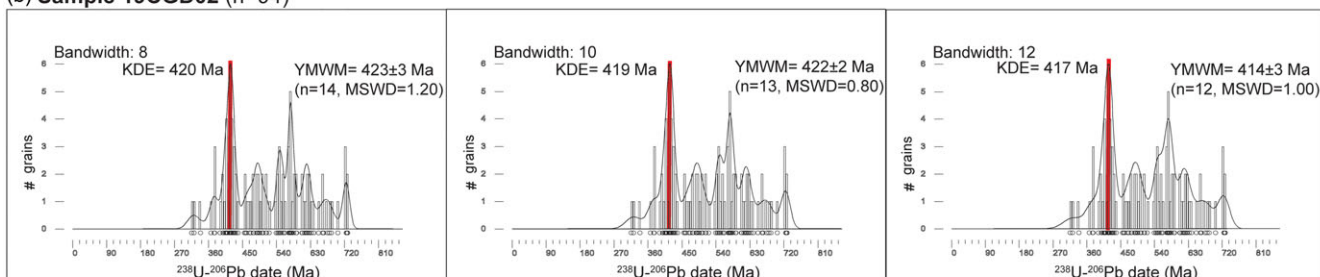
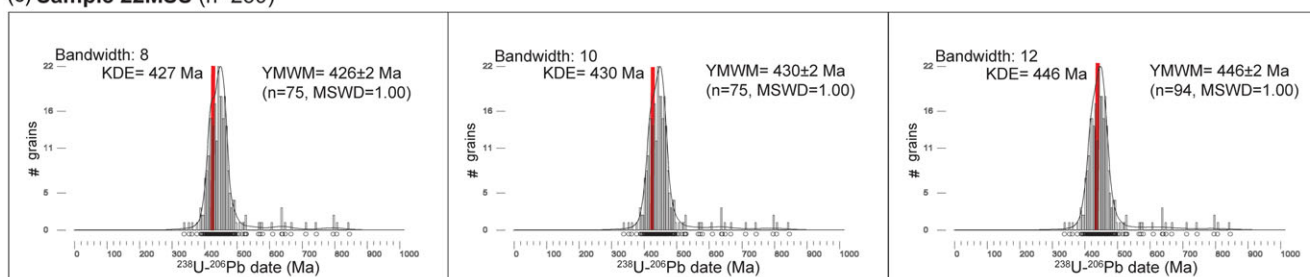


Figure 7. LA-ICP-MS ^{238}U - ^{206}Pb zircon dates with ($\pm 2\sigma$) uncertainties kernel density estimation (KDE) distribution plots up to 900 Ma from 10% discordance filter dataset with various bandwidth values (8, 10, 12) and consistent bin size of 5. Red line represents KDE peak date utilized for youngest mode weighted mean (YMWM) MDA calculation. (a) Sample 19CH01. (b) Sample 19CGD02 (c) sample 22MSS.

Table 2. X-ray diffraction (XRD) mineralogical analyses of this study's samples

Sample	Quartz	K-spar	Plagioclase	Chlorite	Kaolinite	Illite/Mica	Total wt.%
19CH01	55	3	9	8	0	25	100
19CGD02	39	3	8	9	1	40	100
22MSS	41	2	1	9	1	46	100

(a) Sample 19CH01 (n=200)**(b) Sample 19CGD02 (n=94)****(c) Sample 22MSS (n=259)****Figure 8.** LA-ICP-MS ^{238}U - ^{206}Pb zircon dates with ($\pm 2\sigma$) uncertainties kernel density estimation (KDE) distribution plots up to 900 Ma from common Pb-corrected (^{207}Pb method) dataset with various bandwidth values (8, 10, 12) and consistent bin size of 5. Red line represents KDE peak date utilized for youngest mode weighted mean (YMWM) MDA calculation. (a) Sample 19CH01. (b) Sample 19CGD02 (c) sample 22MSS.

Utilizing the common Pb correction for the ^{238}U - ^{206}Pb dates up to 900 Ma presents a total of 200 zircon dates spanning from Precambrian to Devonian (Fig. 6b). The YMWM with various bandwidths provides dates of 427 ± 2 Ma ($n = 24$, $\text{MSWD} = 0.96$, bandwidth = 8), 428 ± 2 Ma ($n = 23$, $\text{MSWD} = 0.97$, bandwidth = 10) and 428 ± 2 Ma ($n = 24$, $\text{MSWD} = 1.00$, bandwidth = 12) (Fig. 8a). The elemental (XRF) analyses of sample 19CH01 exhibit a major element composition marked by high Si, intermediate Al, and low Ca and Fe, characteristic of siltstone and sandstone lithological facies (supplementary table S2). Mineralogical (XRD) analyses support this observation, demonstrating a composition involving quartz, K-feldspar, plagioclase, chlorite, kaolinite and illite/mica. The corresponding weight percent quantification values are outlined in (Table 2).

4. b. Cwm Graig Ddu, Powys, Wales, UK

Sample 19CGD02 obtained from the Pterinea Beds yielded a total of 65 zircon dates post-application of the $\leq 10\%$ discordance filter. These zircon dates span from the Precambrian to the Devonian for the micaceous flaggy siltstone beds within the Pterinea Beds (Fig. 6a; supplementary table S1). The youngest estimate for this sample is the YSG date of 377 ± 8 Ma (6% disc) and the $\text{YC}2\sigma + 3$ estimation presents a date of 412 ± 6 ($n = 9$, $\text{MSWD} = 2.20$). The YMWM with various bandwidths provides dates of 423 ± 3 Ma ($n = 9$, $\text{MSWD} = 0.80$, bandwidth = 8), 423 ± 3 Ma ($n = 9$, $\text{MSWD} = 0.80$, bandwidth = 10) and 423 ± 3 Ma ($n = 9$, $\text{MSWD} = 0.80$, bandwidth = 12) (Fig. 7b).

Utilizing the common Pb correction for the ^{238}U - ^{206}Pb dates up to 900 Ma presents a total of 94 zircon dates spanning from

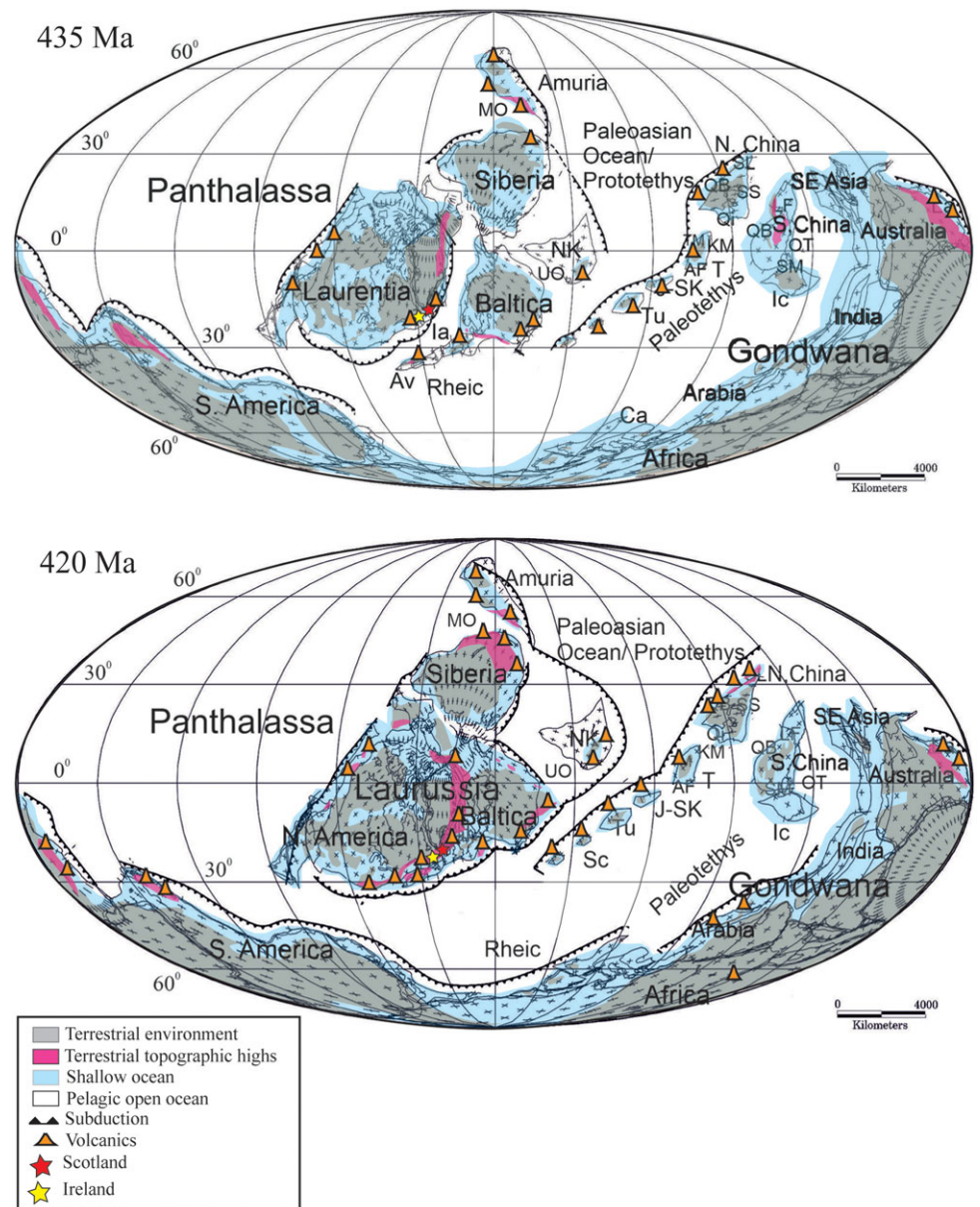


Figure 9. Paleogeographic reconstruction during Early to Late Silurian (after Torsvik & Cocks, 2016 and Golanka *et al.*, 2023). During Early Silurian (435 Ma) closing of the Iapetus Ocean forms volcanic arcs (fore-arc and back-arc) near subduction margins of Laurentia, Baltica and Avalonia, producing widespread tectonic activity (Chew & Strachan, 2014; Garza *et al.*, 2023). By Late Silurian (425 Ma), Caledonian Mountains are formed near an active continental margin producing substantial volcanic activity (Chew & Strachan, 2014; Torsvik & Cocks, 2016; Golanka *et al.*, 2023).

Precambrian to Devonian (Fig. 6b). The YMW with various bandwidths provides dates of 423 ± 3 Ma ($n = 14$, MSWD = 1.20, bandwidth = 8), 422 ± 2 Ma ($n = 13$, MSWD = 0.80, bandwidth = 10) and 414 ± 3 Ma ($n = 12$, MSWD = 1.00, bandwidth = 12) (Fig. 8b). The elemental (XRF) assessments for sample 19CGD02 also depict a major element composition featuring high Si, intermediate Al, and low Ca and Fe, consistent with the siltstone and sandstone lithological facies (supplementary table S2). The mineralogical (XRD) analyses substantiate these findings, revealing a composition akin to quartz, K-feldspar, plagioclase, chlorite, kaolinite and illite/mica, with corresponding weight percent quantification values presented in (Table 2).

4. c. Borrisnoe Mountain, County Tipperary, Ireland

Sample 22MSS obtained from the Hollyford Formation yielded a total of 187 zircon dates post-application of a $\leq 10\%$ discordance filter. These zircon dates span from the Precambrian to the Devonian age range for the micaceous siltstone bed within the

Hollyford Formation (Fig. 6a; supplementary table S1). Among the estimations derived from the U-Pb LA-ICP-MS dates for sample 22MSS, the youngest estimate is the YSG date of 377 ± 13 Ma (4% disc) and the YC2 σ + 3 estimation presents a date of 390 ± 13 Ma ($n = 4$, MSWD = 2.00). Additionally, the YMW with various bandwidths provides dates of 424 ± 3 Ma ($n = 25$, MSWD = 0.98, bandwidth = 8), 424 ± 3 Ma ($n = 25$, MSWD = 0.98, bandwidth = 10) and 431 ± 3 Ma ($n = 21$, MSWD = 1.00, bandwidth = 12) (Fig. 7c).

Utilizing the common Pb correction for the ^{238}U - ^{206}Pb dates up to 900 Ma yields a total of 259 zircon dates spanning from Precambrian to Devonian. (Fig. 6b). The YMW with various bandwidths provides dates of 426 ± 2 Ma ($n = 75$, MSWD = 1.00, bandwidth = 8), 430 ± 2 Ma ($n = 75$, MSWD = 1.00, bandwidth = 10) and 446 ± 2 Ma ($n = 94$, MSWD = 1.00, bandwidth = 12) (Fig. 8c). Elemental analyses (XRF) of sample 22MSS reveal a major element composition characterized by high Si, intermediate Al, and low Ca and Fe, indicative of siltstone and sandstone lithological facies (supplementary table S2). Mineralogical analyses (XRD) align with the elemental data, confirming a composition

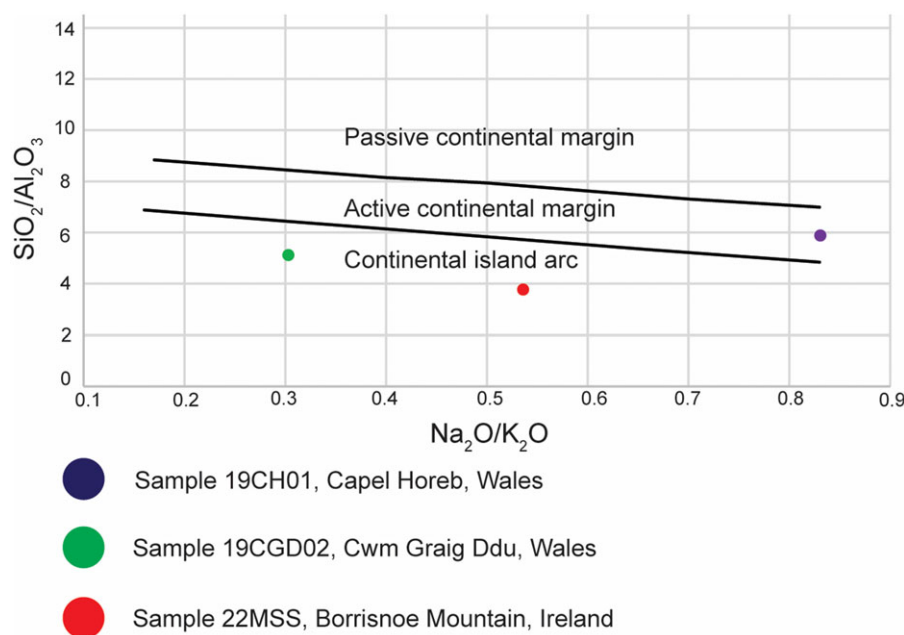


Figure 10. Tectonic setting discrimination diagram based on XRF major element composition (after Roser & Korsch, 1986 and Sahraeyan *et al.* 2015).

comprising quartz, K-feldspar, plagioclase, chlorite, kaolinite and illite/mica. Corresponding weight percent quantification values are detailed in (Table 2).

5. Discussion

5. a. Geochemistry of tectonic setting sediment provenance

The closure of the Iapetus Ocean resulted from the collision between Laurentia, Baltica and Avalonia during the Early Ordovician to the Late Silurian, leading to significant tectonism and the formation of the Caledonian Mountains (Chew & Strachan, 2014; Torsvik & Cocks, 2016; Golanka *et al.*, 2023; Garza *et al.*, 2023). Deposits containing *Cooksonia* macrofossils, investigated in this study and located in Wales and Ireland, originated from island arcs in the Early Silurian, transitioning to volcanic and plutonic sources from an active continental margin by the Late Silurian (Fig. 9) (Chew & Strachan, 2014; Torsvik & Cocks, 2016; Golanka *et al.*, 2023).

The XRF elemental analyses conducted in this study on three siltstone samples from distinct localities validate the paleo-continental reconstructions (Fig. 10). Our findings reveal significant island arc sediment contributions for samples 22MSS and 19CGD02, collected from Borrisnoe Mountain (Ireland) and Cwm Graig Ddu (Wales). Conversely, sample 19CH01, originating from Capel Horeb (Wales), exhibits predominant sediment input from an active continental margin.

The XRD mineralogical analyses align with the typical siltstone mineralogy, predominantly composed of quartz and feldspars, with a noticeable clay component primarily represented by illite/mica (Table 2). This dataset is particularly valuable as it corresponds with previous lithological descriptions of rocks enclosing the *Cooksonia* macrofossils across the three different localities (Heard, 1939; Straw, 1952; Cope, 1959; Potter & Price, 1965; Edwards & Davies, 1976; Edwards *et al.*, 1979; Edwards & Feehan, 1980; Edwards *et al.*, 1983). The main distinctions among localities lie in the mineral composition of tectosilicates and clays. Borrisnoe Mountain (Ireland) and Cwm Graig Ddu (Wales) exhibit a very similar mineral composition in tectosilicates and clays, supporting our elemental data indicating a comparable

sediment source (Table 2). In contrast, Capel Horeb (Wales) contains a higher tectosilicate content and significantly lower clay content, suggesting a distinct sediment source.

5. b. Implications for assigning MDAs

MDAs derived from detrital zircons, typically adhere to the 'law of detrital zircon', a principle asserting that a geological formation or rock bed cannot be older than its youngest constituent, but can be younger. This principle sets a threshold age limit for MDAs (Gehrels, 2014; Herriott *et al.*, 2019; Sharman & Malkowski, 2020; Brookfield *et al.*, 2021). When evaluating MDAs for the samples in this study using the 10% discordance-filtered U-Pb dates, interpretations using the YSG and youngest cluster of three or more grains overlapping at two sigma ($\text{YC}2\sigma + 3$) methods reveal U-Pb dates significantly younger than their presently assessed ages for all samples (Fig. 6a). However, MDA methodologies such as the YSG and $\text{YC}2\sigma + 3$ methods might be considered less conservative, as they rely on the youngest concordant zircons or clusters, potentially yielding considerably younger dates than the true depositional age (TDA) due to potential Pb loss or systematic uncertainties (Coutts *et al.*, 2019; Andersen *et al.*, 2019; Herriott *et al.*, 2019; Garza *et al.*, 2023; Sharman and Malkowski, 2024).

The YMWM dates derived from the 10% discordance-filtered U-Pb dates generally match the biostratigraphy age within a certain range of uncertainty, except for sample 19CH01 (Fig. 7). In this particular case, the KDE plots produced YMWM dates that either skewed too young or too old compared to the biostratigraphy age. Despite the current assigned biostratigraphy age for sample 19CH01 being Ludfordian–Gorstian (~423–426 Ma), the KDE with a bandwidth of 8 generated a younger YMWM date of 408 ± 7 Ma ($n = 5$, $\text{MSWD} = 1.80$), while the KDE with a bandwidth of 10 also yielded a YMWM date of 408 ± 7 Ma ($n = 5$, $\text{MSWD} = 1.80$) (Fig. 7a). Conversely, the KDE with a bandwidth of 12 resulted in an older YMWM date of 436 ± 3 Ma ($n = 14$, $\text{MSWD} = 1.00$). This discrepancy in YMWM dates seems to be driven by Pb loss and the variability in selected bandwidths used for KDE plots.

The consistently younger dates obtained through the YSG, $\text{YC}2\sigma + 3$ and YMWM methods, in comparison to their assigned

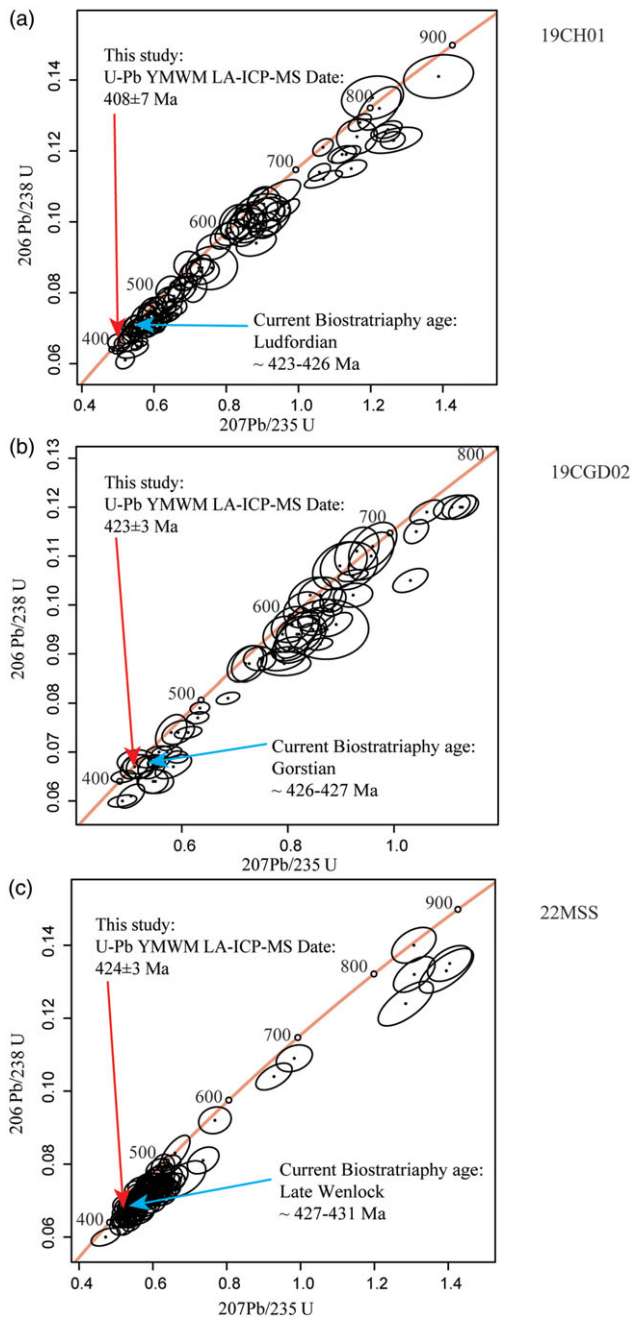


Figure 11. ^{238}U - ^{206}Pb LA-ICP-MS concordia diagrams reported as total Pb with 10% discordance filter for zircons younger than 900 Ma from this study's localities in Ireland and Wales. (a) Sample 19CH01 from Capel Horeb, Wales, accepted biostratigraphy age from Edwards & Richardson (2004), Edwards & Kenrick (2015). (b) Sample 19CGD02 from Cwm Graig Ddu, Wales, accepted biostratigraphy age from Edwards & Richardson (2004), Edwards & Kenrick (2015). (c) Sample 22MSS from Borrisnoe Mountain, Ireland, accepted biostratigraphy age from Edwards & Feehan (1980), Edwards *et al.* (1983), Edwards & Kenrick (2015), Salamon *et al.* (2018). Black ovals present LA-ICP-MS dates with 2σ uncertainty, blue arrow shows accepted biostratigraphy age and red arrow displays the YMWMS MDA from dataset with 10% discordance filter.

biostratigraphic age, may be attributed to significant disturbances in the U-Pb system within the samples. As outlined in the methods section, only 49% of the total zircons (378 out of 787) met the criteria for the 10% discordance filter, indicating Pb loss within the zircons across all three fossil sites. The concordia diagrams illustrate Pb loss within the three samples, especially the youngest grains (Fig. 11). Figure 9 illustrates substantial tectonic activity in

the three localities due to the collision of Baltica, Avalonia and Laurentia, leading to the formation of the Caledonian Mountains from the Early Ordovician to the Late Silurian. This tectonic activity likely induced zircon metamictization and subsequent Pb loss (Chew & Strachan, 2014; Torsvik & Cocks, 2016; Glonka *et al.*, 2023; Garza *et al.*, 2023). Additionally, during the Late Devonian through the Early Carboniferous, the collision between Laurentia (now Laurussia) and Gondwana contributed to the formation of Pangea, potentially exacerbating the degree of metamictization in the already affected zircon grains (Blakey, 2003; Blakey, 2008).

According to Vermeesch (2012), the choice of kernel in KDE plots is less critical compared to the bandwidth. Depending on the selected bandwidth, KDE diagrams may be oversmoothed or under-smoothed, potentially biasing MDA calculations and resulting in younger or older U-Pb dates. In datasets with limited available data, a larger bandwidth is employed, resulting in a smoother KDE plot. Conversely, in datasets with abundant data, a narrower bandwidth is utilized to maintain high resolution in KDE plots, ensuring that the peaks in the KDE distributions are not oversmoothed (Vermeesch, 2012). However, discrepancy arises from the non-standardized use of different bandwidth values across the geochronology community, where bandwidth value selection can vary between laboratories or individuals, leading to potential inconsistencies in sediment provenance results or MDA calculations.

When utilizing the common Pb-corrected (^{207}Pb method) ^{238}U - ^{206}Pb dates up to 900 Ma to compute YMWMS dates with different bandwidths, we also observe variations in the YMWMS dates (Fig. 8). The advantage of employing this common Pb-corrected method is its incorporation of more U-Pb dates into statistical calculations for MDAs that might have otherwise been discarded during the filtering process. However, since the common Pb correction does not filter based on discordance but rather shifts all ^{238}U - ^{206}Pb zircon dates including the discordant grains with Pb-loss to concordia, we attribute the variation in YMWMS dates to the different bandwidth values.

For instance, in the case of sample 19CH01, with a Ludfordian–Gorstian biostratigraphy age (~423–426 Ma), the YMWMS dates generated with bandwidths of 8, 10 and 12 all fell within the uncertainty range of the biostratigraphy age (Fig. 8a). The KDE with a bandwidth of 8 produced a YMWMS date of 427 ± 2 Ma ($n = 24$, MSWD = 0.96), while the KDE with a bandwidth of 10 yielded a YMWMS date of 428 ± 2 Ma ($n = 23$, MSWD = 0.97), and the KDE with a bandwidth of 12 resulted in a YMWMS date of 428 ± 2 Ma ($n = 24$, MSWD = 1.00).

Sample 19CGD02, with a Gorstian biostratigraphy age (~426–427 Ma), exhibited the most variability, with only the YMWMS date generated using a bandwidth value of 8 matching the biostratigraphy age within uncertainty (Fig. 8b). The KDE with a bandwidth of 8 yielded a YMWMS date of 423 ± 3 Ma ($n = 14$, MSWD = 1.20), while the KDE with a bandwidth of 10 resulted in a YMWMS date of 422 ± 2 Ma ($n = 13$, MSWD = 0.80), and the KDE with a bandwidth of 12 produced a significantly younger YMWMS date of 414 ± 3 Ma ($n = 12$, MSWD = 1.00).

Sample 22MSS, with a Homeric–Sheinwoodian biostratigraphy age (~427–431 Ma), displayed some variability, with the YMWMS dates generated using bandwidths of 8 and 10 matching the biostratigraphy age within uncertainty, while the YMWMS date with a bandwidth of 12 resulted in a significantly older date (Fig. 8c). The KDE with a bandwidth of 8 yielded a YMWMS date of 426 ± 2 Ma ($n = 75$, MSWD = 1.00), while the KDE with a bandwidth of 10 produced a YMWMS date of 430 ± 2 Ma ($n = 75$,

Table 3. Comparison of ^{238}U - ^{206}Pb LA-ICP-MS youngest mode weighted mean (YMWM) MDA calculations using a 10% discordance filter, a common Pb correction (^{207}Pb method) and various KDE bandwidth values (Bw) with assigned biostratigraphy age

Sample	Bin size	Bw	Calculated with 10%-disc filter			Calculated with Common Pb correction			Biostratigraphy age
			KDE	YMWM	n = and MSWD	KDE	YMWM	n = and MSWD	
22MSS	5	8	423	424 ± 3	(n = 25, MSWD = 0.98)	427	426 ± 2	(n = 75, MSWD = 1.00)	427–431 Ma
	5	10	425	424 ± 3	(n = 25, MSWD = 0.98)	430	430 ± 2	(n = 75, MSWD = 1.00)	427–431 Ma
	5	12	430	431 ± 3	(n = 21, MSWD = 1.00)	446	446 ± 2	(n = 94, MSWD = 1.00)	427–431 Ma
19CGD02	5	8	421	423 ± 3	(n = 9, MSWD = 0.80)	420	423 ± 3	(n = 14, MSWD = 1.20)	426–427 Ma
	5	10	421	423 ± 3	(n = 9, MSWD = 0.80)	419	422 ± 2	(n = 13, MSWD = 0.80)	426–427 Ma
	5	12	420	423 ± 3	(n = 9, MSWD = 0.80)	417	414 ± 3	(n = 12, MSWD = 1.00)	426–427 Ma
19CH01	5	8	414	408 ± 7	(n = 5, MSWD = 1.80)	426	427 ± 2	(n = 24, MSWD = 0.96)	423–426 Ma
	5	10	413	408 ± 7	(n = 5, MSWD = 1.80)	427	428 ± 2	(n = 23, MSWD = 0.97)	423–426 Ma
	5	12	440	436 ± 3	(n = 14, MSWD = 1.00)	428	428 ± 2	(n = 24, MSWD = 1.00)	423–426 Ma

MSWD = 1.00), and the KDE with a bandwidth of 12 resulted in a significantly older YMWM date of 446 ± 2 Ma (n = 94, MSWD = 1.00).

Overall, we recognized that Pb loss may be at play when not using the common Pb correction, so to account for this, we thermally annealed our grains and applied a more stringent 10% discordance filter for one of our interpretation methods. Furthermore, we use a more conservative YMWM MDA interpretation instead of relying on the YSG and $\text{YC}2\sigma + 3$, which are more prone to erroneous interpretations in samples impacted by cryptic Pb loss. Discordance alone proves insufficient for identifying Pb loss in Phanerozoic LA-ICP-MS data, as the effects of Pb loss may be cryptic or occur shortly after crystallization, leading to U-Pb analyses shifting along concordia (Andersen *et al.*, 2019; Garza *et al.*, 2023; Sharman and Malkowski, 2024). This issue remains undetectable in relatively low-precision LA-ICP-MS analyses (Andersen *et al.*, 2019).

The YMWM MDA approach, coupled with the common Pb correction (^{207}Pb method) and a bandwidth of 8, consistently produces dates that closely approximate the current assessed biostratigraphy ages for Borrisnoe Mountain, Ireland (sample 22MSS), Cwm Graig Ddu Quarry, Wales (sample 19CGD02), and Capel Horeb, Wales (sample 19CH01) (Table 3). We opted for the YMWM MDAs with a bandwidth of 8 due to its ability to generate KDE plots with higher resolutions that avoid oversmoothing KDE distribution peaks (Vermeesch, 2012). However, the discrepancies arising from the use of different bandwidth values for KDE plots, whether with discordance-filtered or common Pb-corrected data, require careful evaluation. Bandwidth value preferences vary among labs and individuals, potentially leading to MDA interpretation biases.

Ultimately, the most accurate LA-ICP-MS MDA estimates appear consistent with U-Pb Chemical Abrasion-Isotope Dilution-Thermal Ionization Mass Spectrometry (CA-ID-TIMS) dates are derived from calculations involving averages rather than solely relying on the youngest grains (Herriott *et al.*, 2019; Tian *et al.*, 2022; Garza *et al.*, 2023). CA-ID-TIMS is the most precise and accurate U-Pb dating technique, boasting $\leq 0.1\%$ 2σ age precision (Mattinson, 2005; Bowring *et al.*, 2006; Schaltegger *et al.*, 2015). This approach helps minimize the effects of potential Pb loss (Herriott *et al.*, 2019; Tian *et al.*, 2022; Garza *et al.*, 2023). Given these considerations, we endorse the YMWM MDA method with

the common Pb correction as the most suitable option for this study, given its alignment with CA-ID-TIMS results in other studies (Tian *et al.*, 2022; Garza *et al.*, 2023). Moreover, it has previously demonstrated effectiveness in yielding optimal age results when applied to Early Paleozoic zircon grains (Tian *et al.*, 2022; Garza *et al.*, 2023).

5. c. Implications for the refinement of *Cooksonia* ages

The determination of where and when the earliest vascular plants originated is critical for understanding the emergence of land biomes and the broader development of the biosphere. This knowledge is crucial for unraveling the adaptations that shaped vascular plants and understanding the intricate ecological interactions that facilitated the terrestrial colonization by the first arthropods (Shear & Selden, 2001; Gerrienne *et al.*, 2016; Brookfield *et al.*, 2021; Brookfield *et al.*, 2022; Dahl & Arens, 2020). Molecular phylogenies of vascular plants suggest that *Cooksonia* evolved during the Middle Cambrian (Rota-Stabelli *et al.*, 2013; Morris *et al.*, 2018). However, macrofossils of the earliest vascular plants are exclusively found in the Silurian period (Shear & Selden, 2001; Brookfield *et al.*, 2020; Dahl & Arens, 2020). The Silurian is recognized as the terrestrial equivalent of the Cambrian ‘explosion’ of marine faunas, marked by an increase in phenotypic diversity and the establishment of frameworks reminiscent of modern ecosystems (Bateman *et al.*, 1998; Benton & Emerson, 2007; Minter *et al.*, 2017).

Previous studies into the appearance of vascular plants on land have employed molecular clock phylogenetic models, microfossil records (trilete spores) and macrofossil records to understand vascular plants evolution and the timing of land colonization by *Cooksonia* (Edwards & Kenrick, 2015; Salamon *et al.*, 2018; Donoghue *et al.*, 2021). However, these prior assessments encounter discrepancies in ages between the micro- and macrofossil records which rely solely on biostratigraphy for calibration in phylogenetic models (Clarke *et al.*, 2011; Edwards & Kenrick, 2015; Morris *et al.*, 2018; Servais *et al.*, 2019). The primary issue is the exclusive reliance on biostratigraphy for dating both micro- and macrofossils, while a decent starting point, U-Pb dates provides a numerical assessment. Second, there exists a 20-million-year gap between trilete spores dated to a Late Ordovician (Katian) age and the oldest macrofossil assigned to a Middle Silurian (Wenlock) age,

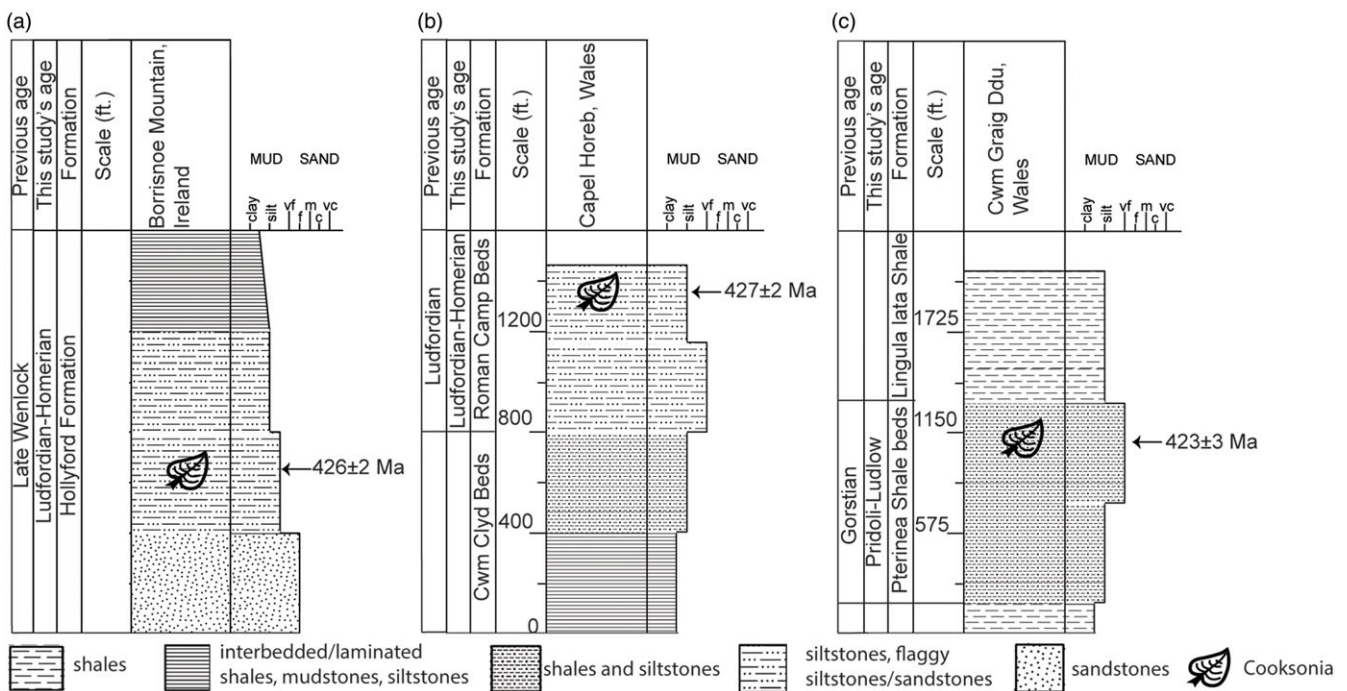


Figure 12. Stratigraphic columns displaying previous and this study's chronostratigraphic assessment. (a) Generalized stratigraphic column of Hollyford Formation at Borrisnoe Mountain, Ireland (Cope, 1959; Edwards & Feehan, 1980; Edwards *et al.*, 1983). LA-ICP-MS YMW dates derive from sample 22MSS. (b) Stratigraphic column of *Pterinea* Shale Beds and *Lingula lata* Shale at Cwm Graig Ddu, Wales (Straw, 1952; Edwards *et al.*, 1979). LA-ICP-MS YMW date is from sample 19CGD02. (c) Stratigraphic column of Cwm Clyd Beds and Roman Camp Beds at Capel Horeb, Wales (Heard, 1939; Potter & Price, 1965; Edwards & Davies, 1976; Edwards & Rogerson, 1979). LA-ICP-MS YMW date derives from sample 19CH01.

creating discordance between the micro- and microfossil records (Edwards & Kenrick, 2015; Salamon *et al.*, 2018). Third, phylogenetic models calibrated by fossils contradict both the micro- and microfossil records, estimating an initial appearance during the Middle Cambrian (Clarke *et al.*, 2011; Morris *et al.*, 2018; Servais *et al.*, 2019). Our study establishes MDAs using detrital zircon ^{238}U - ^{206}Pb and ^{207}Pb - ^{206}Pb LA-ICP-MS dates from the three oldest sites containing *Cooksonia* macrofossils in Wales and Ireland.

The existing order and age assessment of the oldest sites harbouring *Cooksonia* macrofossils characterizes Borrisnoe Mountain, Ireland, as the oldest, assigned a Middle Silurian (Late Wenlock) age, followed by Cwm Graig Ddu Quarry, Wales, designated with a Late Silurian (Gorstian) age, and subsequently Capel Horeb, Wales, attributed to a Late Silurian (Ludfordian) age (Table 1) (Edwards & Davies, 1976; Edwards *et al.*, 1979; Edwards & Rogerson, 1979; Edwards & Feehan, 1980; Edwards *et al.*, 1983; Edwards & Richardson, 2004). However, our recent U-Pb MDA dating outcomes refine these former age assessments. Our new findings reveal that utilizing the YMW MDA with common Pb-corrected ^{238}U - ^{206}Pb zircon dates indicates that both Borrisnoe Mountain and Capel Horeb host the oldest *Cooksonia* macrofossils, with both localities exhibiting a Gorstian–Homerian age for the sediments containing these macrofossils (Fig. 12). Specifically, the Borrisnoe Mountain sediments of the Hollyford Formation yield an MDA of 426 ± 2 Ma, while the Capel Horeb sediments of the Upper Roman Camp Formation provide an MDA of 427 ± 2 Ma (Fig. 13). However, due to the uncertainty inherent in U-Pb LA-ICP-MS analyses, there remains a possibility that the *Cooksonia* macrofossil from Capel Horeb could indeed be the oldest. Therefore, further CA-ID-TIMS analyses are imperative to obtain more precise and accurate U-Pb dates, allowing us to

differentiate between these two sites definitively. In contrast, the Cwm Graig Ddu Quarry site presents a Pridoli-Ludlow MDA age of 423 ± 3 Ma, making it the youngest locality bearing *Cooksonia* macrofossils among the three sites examined in this study (Fig. 13). Notably, this MDA age aligns consistently within uncertainty with its assigned Ludfordian biostratigraphy age (Edwards & Davies, 1976; Edwards & Rogerson, 1979; Edwards & Richardson, 2004; Edwards & Kenrick, 2015).

The MDAs obtained for the localities investigated in this study are crucial in unraveling the evolution of vascular plants and providing valuable insights into broader patterns of biological evolution, including diversification and the environmental factors influencing their development (Kenrick *et al.*, 2012; De Vries & Archibald, 2017). Understanding the age and evolution of *Cooksonia* plays a pivotal role in reconstructing paleoenvironments and offers valuable perspectives on ancient plant life, contributing significantly to changes in biogeochemical cycles, paleoclimates and ecosystems (Wellman, 2010; Clarke *et al.*, 2011; Lenton *et al.*, 2012; Yuan *et al.*, 2023). Refined maximum ages are indispensable for improving phylogenetic models and reconstructing plant evolution and the tree of life (Lenton *et al.*, 2012). The U-Pb MDAs act as a foundational tool for more accurately calibrating molecular clocks, assisting in the estimation of divergence times for different plant lineages.

6. Conclusions

The aim of this study is to reassess the chronological placement of the *Cooksonia* genus by employing U-Pb dating on the oldest macrofossils discovered in Wales (UK) and Ireland. The evolution of vascular plants on land has been a dynamic process marked by numerous innovations and adaptations, playing a pivotal role in

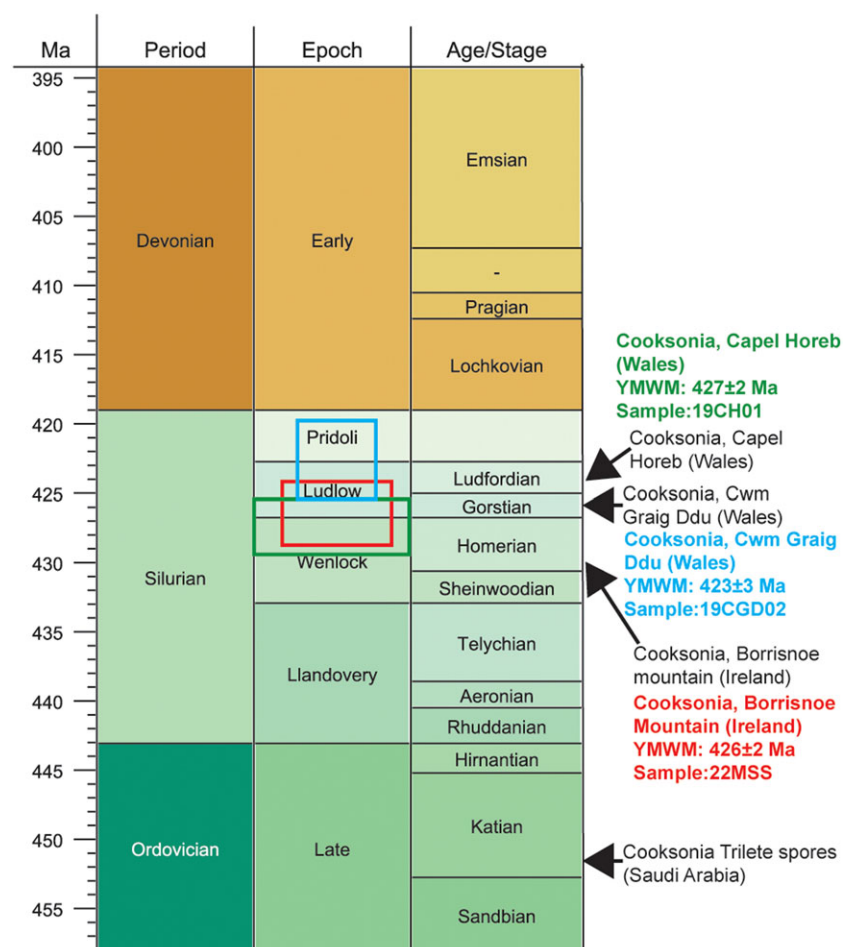


Figure 13. Geological time scale with *Cooksonia*'s first appearance datum (FAD) micro- and macrofossil record. Current assigned biostratigraphy age (darker font) (from Edwards *et al.*, 1979; Edwards & Rogerson, 1979; Edwards & Feehan, 1980; Edwards *et al.*, 1983; Edwards & Richardson, 2004; Edwards & Kenrick, 2015; Salamon *et al.*, 2018). This study's ^{238}U - ^{206}Pb (common Pb-corrected) youngest mode weighted mean (YMWM) are shown in colour font and boxes. Borrisnoe Mountain (Ireland) in red; Cwm Graig Ddu (Wales) in blue; Capel Horeb (Wales) in green.

shaping terrestrial environments globally (Kenrick *et al.*, 2012; DeVries & Archibald, 2017). Beyond transforming landscapes, these plants have exerted a profound influence on the evolution of other organisms and ecosystems, establishing themselves as a critical component of the planet's biodiversity and ecological complexity (Garwood & Edgecombe, 2011; Kenrick *et al.*, 2012; Dunlop *et al.*, 2013; Lenton *et al.*, 2016; Wallace *et al.*, 2017; Dahl & Arens, 2020).

This study presents the first ^{238}U - ^{206}Pb and ^{207}Pb - ^{206}Pb zircon dates for the earliest recognized *Cooksonia* macrofossils, adjusting previous age interpretations reliant on biostratigraphy. By leveraging detrital zircon U-Pb dating and the YMWM MDA approach, we systematically refined the age assessments of key fossil sites harbouring *Cooksonia* macrofossils in Ireland and Wales. Our findings present Gorstian–Homerian maximum ages for both the Borrisnoe Mountain (Ireland) and Capel Horeb (Wales) macrofossils, with maximum ages of 426 ± 2 Ma and 427 ± 2 Ma, respectively (Fig. 13). For Cwm Graig Ddu (Wales), our *Cooksonia*'s (Pridoli–Ludlow) MDA of 423 ± 3 Ma aligns with its assigned biostratigraphy (Gorstian) age within the margin of uncertainty. Future U-Pb CA-ID-TIMS analyses are imperative to confirm Pb loss within the zircon grains in these localities and produce more accurate and precise U-Pb dates.

This study's U-Pb LA-ICP-MS dataset was examined in two different ways: first, with a 10% discordance filter, and second, with common Pb correction using the ^{207}Pb method, while varying the bandwidth values. This analysis revealed biases when calculating MDAs using statistical approaches reliant on KDE distributions (Figs. 7 & 8). To mitigate these biases, we suggest using lower

bandwidth values to generate KDEs with higher resolution, avoiding oversmoothing KDE distribution peaks. Furthermore, elemental and mineralogical analyses conducted on our samples validate paleo-continental reconstructions (Fig. 10). Specifically, they indicate island arc sediment contributions for Borrisnoe Mountain in Ireland and Cwm Graig Ddu in Wales. In contrast, Capel Horeb in Wales shows sediment input from an active continental margin. The findings significantly contribute to the understanding of tectonic settings during the Silurian, and the refined U-Pb MDAs can assist adjusting the tree of life by providing a more precise calibration of molecular clocks and estimating divergence times for various plant lineages.

Supplementary material. The supplementary material for this article can be found at <https://doi.org/10.1017/S0016756824000384>

Acknowledgements. Data supporting the conclusions can be obtained from the supplementary material (supplementary tables S1, S2) and will be placed in the Cambridge University Press Supplementary Material data archive. We appreciate funding for this work by the Geological Society of America Graduate Student Specialized Grant from the Charles A. & June R.P. Ross Research Fund, and a Student Research Award from the University of Texas at Austin (UT Austin) Center for Planetary Systems Habitability. U-Pb dates were collected at the JSG UTChron Laboratory at UT Austin. We appreciate analytical assistance by L. Stockli and comments from L. Boucher and J. Clarke. We appreciate comments from two anonymous reviewers. We thank Coillte, Ben Evans from the British Institute for Geological Conservation and Christina Byrne from Natural Resources Wales for permission to responsibly sample the localities for this study.

Competing interests. The author(s) declare none.

References

- Allen CM, Campbell IH (2012) Identification and elimination of a matrix-induced systematic error in LA-ICP-MS $^{206}\text{Pb}/^{238}\text{U}$ dating of zircon. *Chemical Geology* **332**, 157–65.
- Andersen T (2002) Correction of common lead in U–Pb analyses that do not report ^{204}Pb . *Chemical Geology* **192**, 59–79.
- Andersen T, Elburg MA and Magwaza BN (2019) Sources of bias in detrital zircon geochronology: Discordance, concealed lead loss and common lead correction. *Earth-Science Reviews* **197**, 1–15.
- Archer JB (1981) The Lower Palaeozoic rocks of the northwestern part of the Devilsbit-Keeper Hill Inlier and their implications for the postulated course of the Iapetus Suture Zone in Ireland. *Journal of Earth Sciences* **4**, 21–38.
- Bateman RM, Crane PR, DiMichele WA, Kenrick PR, Rowe NP, Speck T and Stein WE (1998) Early evolution of land plants: phylogeny, physiology, and ecology of the primary terrestrial radiation. *Annual Review of Ecology and Systematics* **1**, 263–92.
- Benton MJ and Emerson BC (2007). How did life become so diverse? The dynamics of diversification according to the fossil record and molecular phylogenetics. *Paleontology* **1**, 23–40.
- Blakey RC (2003) Carboniferous–Permian paleogeography of the assembly of Pangaea. In: *Proceedings of the XVth International Congress on Carboniferous and Permian Stratigraphy* The Wong (ed.), pp. 443–56. Utrecht: Royal Netherlands Academy of Arts and Sciences.
- Blakey RC, Fielding CR, Frank TD, Isbell JL (2008) Gondwana paleogeography from assembly to breakup—A 500 my odyssey. *Geological Society of America Special Papers* **441**, 1–28.
- Bowring SA, Schoene B, Crowley JL, Ramezani J and Condon DJ (2006) High-precision U–Pb zircon geochronology and the stratigraphic record: Progress and promise. *The Paleontological Society Papers* **12**, 25–45.
- Brookfield ME, Catlos EJ and Suarez SE (2021) Myriapod divergence times differ between molecular clock and fossil evidence: U/Pb zircon ages of the earliest fossil millipede-bearing sediments and their significance. *Historical Biology* **33**, 2009–13.
- Brookfield ME, Catlos EJ and Suarez SE (2022) Vertebrate lies? Arthropods were the first land animals!. *Geology Today* **2**, 200–16.
- Chew DM, Sylvester PJ and Tubrett MN (2011) U–Pb and Th–Pb dating of apatite by LA-ICPMS. *Chemical Geology* **200**, 1–16.
- Chew DM, Petrus JA and Kamber BS (2014) U–Pb LA-ICPMS dating using accessory mineral standards with variable common Pb. *Chemical Geology* **363**, 185–99.
- Chew DM and Strachan RA (2014) The Laurentian caledonides of Scotland and Ireland. *Geological Society, London, Special Publications* **390**, 45–91.
- Clarke JT, Warnock RC and Donoghue PC (2011) Establishing a time-scale for plant evolution. *New Phytologist* **192**, 266–301.
- Cleal CJ and Thomas BA (1995) *Palaeozoic Palaeobotany of Great Britain*. London: Chapman and Hall, (Geol. Conserv. Rev., 9).
- Cope RN (1954) Cyrtograptids and retiolitids from County Tipperary. *Geological Magazine* **91**, 319–24.
- Cope RN (1959) The Silurian Rocks of the Devilsbit Mountain District, County. *Proceedings of the Royal Irish Academy. Section B: Biological, Geological, and Chemical Science* **60**, 217–42.
- Coutts DS, Matthews WA and Hubbard SM (2019) Assessment of widely used methods to derive depositional ages from detrital zircon populations. *Geoscience Frontiers* **4**, 1421–35.
- Dahl TW and Arens SK (2020) The impacts of land plant evolution on Earth's climate and oxygenation state—An interdisciplinary review. *Chemical Geology* **547**, 1–25.
- De Vries J and Archibald JM (2018) Plant evolution: landmarks on the path to terrestrial life. *New Phytologist* **217**, 1428–34.
- Dickinson WR and Gehrels GE (2009) Use of U–Pb ages of detrital zircons to infer maximum depositional ages of strata: a test against a Colorado Plateau Mesozoic database. *Earth and Planetary Science Letters* **288**, 115–25.
- Donoghue PC, Harrison CJ, Paps J, Schneider H (2021) The evolutionary emergence of land plants. *Current Biology* **31**, 1281–98.
- Doran RJ (1974) The Silurian rocks of the southern part of the Slieve Phelim inlier, Co. Tipperary. *Proceedings of the Royal Irish Academy. Section B: Biological, Geological, and Chemical Science* **74**, 193–202.
- Dunlop JA, Scholtz G and Selden PA (2013) Water-to-land transitions. In *Arthropod biology and evolution: molecules, development, morphology*. (eds. Minelli A, Boxshall G, Fusco G.), pp. 417–39. Berlin, Heidelberg: Springer Berlin Heidelberg, Print.
- Edwards D and Davies EC (1976) Oldest recorded in situ tracheids. *Nature* **263**, 494–95.
- Edwards D and Rogerson EC (1979) New records of fertile Rhyniophytina from the late Silurian of Wales. *Geological Magazine* **116**, 93–98.
- Edwards D, Bassett MG and Rogerson CW (1979) The earliest vascular land plants: continuing the search for proof. *Lethaia*, **12**, 313–24.
- Edwards D and Feehan J (1980) Records of Cooksonia-type sporangia from late Wenlock strata in Ireland. *Nature* **287**, 41–42.
- Edwards D (1982) Fragmentary non-vascular plant microfossils from the late Silurian of Wales. *Botanical Journal of the Linnean Society* **84**, 223–56.
- Edwards D, Feehan J and Smith DG (1983) A late Wenlock flora from Co. Tipperary, Ireland. *Botanical Journal of the Linnean Society*, **86**, 19–36.
- Edwards D and Richardson JB (2004) Silurian and Lower Devonian plant assemblages from the Anglo-Welsh Basin: a palaeobotanical and palynological synthesis. *Geological Journal* **39**, 375–402.
- Edwards D, Morris JL, Richardson JB and Kenrick P (2014) Cryptospores and cryptophytes reveal hidden diversity in early land floras. *New Phytologist* **202**, 50–78.
- Edwards D and Kenrick P (2015) The early evolution of land plants, from fossils to genomics: a commentary on Lang (1937)'On the plant-remains from the Downtonian of England and Wales'. *Philosophical Transactions of the Royal Society B: Biological Sciences*, **370**, 1–12.
- Fairey BJ, Kerrison A, Meere PA, Mulchrone KF, Hofmann M, Gärtner A, Sonntag BL, Linnemann U, Kuiper KF, Ennis M, Mark C (2018) The provenance of the Devonian Old Red Sandstone of the Dingle Peninsula, SW Ireland; the earliest record of Laurentian and peri-Gondwanan sediment mixing in Ireland. *Journal of the Geological Society* **175**, 411–24.
- Finney S and Chen X (1990) The relationship of Ordovician graptolite provincialism to palaeogeography. *Geological Society, London, Memoirs* **12**, 123–8.
- Garwood RJ and Edgecombe GD (2011) Early terrestrial animals, evolution, and uncertainty. *Evolution: Education and Outreach* **4**, 489–501.
- Garza HK, Catlos EJ, Chamberlain KR, Suarez SE, Brookfield ME, Stockli DF and Batchelor RA (2023) How old is the Ordovician–Silurian boundary at Dob's Linn, Scotland? Integrating LA-ICP-MS and CA-ID-TIMS U–Pb zircon dates. *Geological Magazine* **160**, 1775–89.
- Gehrels G (2014) Detrital zircon U–Pb geochronology applied to tectonics. *Annual Review of Earth and Planetary Sciences* **42**, 127–49.
- Gerrienne P, Servais T and Vecoli M (2016) Plant evolution and terrestrialization during Palaeozoic times—the phylogenetic context. *Review of Palaeobotany and Palynology* **227**, 4–18.
- Golonka J, Porębski SJ and Waśkowska A (2023) Silurian paleogeography in the framework of global plate tectonics. *Palaeogeography, Palaeoclimatology, Palaeoecology* **622**, 1–24.
- Heard A (1939) Further notes on Lower Devonian plants from south Wales. *Quarterly Journal of the Geological Society* **95**, 223–29.
- Herriott TM, Crowley JL, Schmitz MD, Wartes MA and Gillis RJ (2019) Exploring the law of detrital zircon: LA-ICP-MS and CA-TIMS geochronology of Jurassic forearc strata, Cook Inlet, Alaska, USA. *Geology* **47**, 1044–48.
- Jackson SE, Pearson NJ, Griffin WL and Belousova A (2004) The application of laser ablation-inductively coupled plasma-mass spectrometry to in situ U–Pb zircon geochronology. *Chemical Geology* **211**, 47–69.
- Kenrick P, Wellman CH, Schneider H and Edgecombe GD (2012) A timeline for terrestrialization: consequences for the carbon cycle in the Palaeozoic. *Philosophical Transactions of the Royal Society B: Biological Sciences* **367**, 519–36.
- Lane PD (2000) The Pridoli Series. In *British Silurian Stratigraphy* (ed LP Thomas), pp. 429–58. Joint Nature Conservation Committee, Print.
- Lenton TM, Croucher M, Johnson M, Pires N and Dolan L (2012) First plants cooled the Ordovician. *Nature Geoscience* **5**, 86–89.

- Lenton TM, Dahl TW, Daines SJ, Mills BJ, Ozaki K, Saltzman MR and Porada P (2016) Earliest land plants created modern levels of atmospheric oxygen. *Proceedings of the National Academy of Sciences* **113**; 9704–09.
- Ludwig KR and Mundil R (2002) Extracting reliable U-Pb ages and errors from complex populations of zircons from Phanerozoic tuffs. *Geochimica et Cosmochimica Acta* **66**, 463.
- Ludwig K (2008) Isoplot version 4.15: a geochronological toolkit for microsoft Excel. *Berkeley Geochronology Center, Special Publication* **4**, 247–70.
- Mattinson JM (2005) Zircon U-Pb chemical abrasion (“CA-TIMS”) method: combined annealing and multi-step partial dissolution analysis for improved precision and accuracy of zircon ages. *Chemical Geology* **220**, 47–66.
- Melchin MJ, Sadler PM and Cramer BD (2020) The silurian period. In *Geologic Time Scale 2020* (eds Fm Gradstein, JG Ogg, MD Schmitz and GM Ogg), pp. 695–732. Amsterdam, Netherlands: Elsevier, Print.
- Minter NJ, Buatois LA, Mángano MG, Davies NS, Gibling MR, MacNaughton RB and Labandeira CC (2017) Early bursts of diversification defined the faunal colonization of land. *Nature Ecology & Evolution* **1**, 1–10.
- Morris JL, Wright VP and Edwards D (2012) Siluro-Devonian landscapes of southern Britain: the stability and nature of early vascular plant habitats. *Journal of the Geological Society* **169**, 173–90.
- Morris JL, Puttick MN, Clark JW, Edwards D, Kenrick P, Pressel S, Wellman CH, Yang Z, Schneider H and Donoghue PC (2018) The timescale of early land plant evolution. *Proceedings of the National Academy of Sciences* **115**, 2274–83.
- Pogson DJ (2009) The Siluro-Devonian geological time scale: a critical review and interim revision. *Quarterly Notes of the Geological Survey of New South Wales* **130**, 1–13.
- Potter JF and Price JH (1965) Comparative sections through rocks of Ludlovian-Downtonian age in the Llandovery and Llandeilo districts. *Proceedings of the Geologists Association* **76**, 379–402.
- Renzaglia KS, Crandall-Stotler B, Pressel S, Duckett JG, Schuette S and Strother PK (2015a) Permanent spore dyads are not ‘a thing of the past’: on their occurrence in the liverwort *Haplomitrium* (Haplomitriopsida). *Botanical Journal of the Linnean Society* **179**, 658–69.
- Renzaglia KS, Lopez RA and Johnson EE (2015b) Callose is integral to the development of permanent tetrads in the liverwort *Sphaerocarpos*. *Planta* **241**, 615–27.
- Rollinson HR and Pease V (2021) *Using geochemical data: to understand geological processes*. Cambridge: Cambridge University Press.
- Roser BP and Korsch RJ (1986). Determination of tectonic setting of sandstone-mudstone suites using SiO₂ content and K₂O/Na₂O ratio. *The Journal of Geology* **94**, 635–50.
- Rota-Stabelli O, Daley AC and Pisani D (2013). Molecular timetrees reveal a Cambrian colonization of land and a new scenario for ecdysozoan evolution. *Current Biology* **23**, 392–98.
- Rowe H, Hughes N and Robinson K (2012) The quantification and application of handheld energy-dispersive x-ray fluorescence (ED-XRF) in mudrock chemostratigraphy and geochemistry. *Chemical geology* **324**, 122–31.
- Salamon MA, Gerrienne P, Steemans P, Gorzelak P, Filipiak P, Le Hérisse A, Florentin P, Cascales- Miñana B, Brachaniec T, Misz-Kennan M, Niedźwiedzki R and Wiesław T (2018) Putative late Ordovician land plants. *New Phytologist* **218**, 1305–09.
- Sahraeyan M, Seif H, Haddad EE, Mohammadzadeh N (2015) Sedimentology and Geochemistry of the Late Miocene–Pliocene Succession in the Fars Interior (SW Iran): Implications on Depositional and Tectonic Setting, Provenance and Paleoweathering in the Zagros Basin (Ch. 5). In *Chemostratigraphy: Concepts, Techniques, and Applications* (ed M. Ramkumar), pp.103–26. Amsterdam: Elsevier.
- Schaltegger U, Schmitt AK and Horstwood MS (2015). U–Th–Pb zircon geochronology by ID-TIMS, SIMS, and laser ablation ICP-MS: Recipes, interpretations, and opportunities. *Chemical Geology* **402**, 89–110.
- Servais T, Cascales-Miñana B, Cleal CJ, Gerrienne P, Harper DA and Neumann M (2019) Revisiting the Great Ordovician Diversification of land plants: Recent data and perspectives. *Palaeogeography, Palaeoclimatology, Palaeoecology* **534**, 1–39.
- Sharman GR, Sharman JP and Sylvester Z (2018) detritalPy: A Python-based toolset for visualizing and analysing detrital geo-thermochronologic data. *The Depositional Record* **4**, 202–15.
- Sharman GR and Malkowski MA (2020) Needles in a haystack: Detrital zircon UPb ages and the maximum depositional age of modern global sediment. *Earth-Science Reviews* **203**, 1–23.
- Sharman GR, Malkowski MA. (2024) Modeling apparent Pb loss in zircon U–Pb geochronology. *Geochronology* **6**, 37–51.
- Shear WA and Selden PA (2001) 3 Rustling in the undergrowth: animals in early terrestrial ecosystems. In *Plants Invade the Land: Evolutionary and Environmental Perspectives* pp. 29–51. Columbia University Press.
- Sláma J, Košler J, Condon DJ, Crowley JL, Gerdes A, Hanchar JM, Horstwood MSA, Morris GA, Nasdala L, Norberg N, Schaltegger U, Schoene B, Tubrett MN and Whitehouse MJ (2008) Plešovice zircon—a new natural reference material for U–Pb and Hf isotopic microanalysis. *Chemical Geology* **249**, 1–35.
- Steenmans P, Hérisse AL, Melvin J, Miller MA, Paris F, Verniers J and Wellman CH (2009) Origin and radiation of the earliest vascular land plants. *Science* **324**, 353.
- Straw SH (1952) The silurian succession at cwm graig DDU (breconshire). *Geological Journal* **1**, 208–19.
- Strother PK, Al-Hajri S and Traverse A (1996) New evidence for land plants from the lower Middle Ordovician of Saudi Arabia. *Geology* **24**, 55–58.
- Tian H, Fan M, Valencia VA, Chamberlain K, Waite L, Stern RJ and Looke M (2022) Rapid early Permian tectonic reorganization of Laurentia’s plate margins: Evidence from volcanic tuffs in the Permian Basin, USA. *Gondwana Research* **111**, 76–94.
- Torsvik TH and Cocks LRM (2016) *Earth History and Palaeogeography*. Cambridge, UK: Cambridge Univ. Press.
- Verma SP and Armstrong-Altrin JS (2013) New multi-dimensional diagrams for tectonic discrimination of siliciclastic sediments and their application to Precambrian basins. *Chemical Geology* **355**, 117–33.
- Vermeech P (2012). On the visualization of detrital age distributions. *Chemical Geology* **312**, 190–94.
- Wallace MW, Shuster A, Greig A, Planavsky NJ and Reed CP (2017) Oxygenation history of the Neoproterozoic to early Phanerozoic and the rise of land plants. *Earth and Planetary Science Letters* **466**, 12–19.
- Wellman CH and Gray J (2000) The microfossil record of early land plants. *Philosophical Transactions of the Royal Society of London. Series B: Biological Sciences* **355**, 717–32.
- Wellman CH, Osterloff PL and Mohiuddin U (2003) Fragments of the earliest land plants. *Nature* **425**, 282–85.
- Wellman CH (2010) The invasion of the land by plants: when and where?. *The New Phytologist* **188**, 306–09.
- Wellman CH, Steemans P, Vecoli M (2013) Chapter 29 Palaeophytogeography of Ordovician–Silurian land plants. *Geological Society, London, Memoirs* **38**, 461–76.
- White LT and Ireland TR (2012) High-uranium matrix effect in zircon and its implications for SHRIMP U–Pb age determinations. *Chemical Geology* **306**, 78–91.
- Xu H, Wang K, Huang Z, Tang P, Wang Y, Liu B and Yan W (2022) The earliest vascular land plants from the Upper Ordovician of China. *Research Square* **3**, 1–24.
- Yuan W, Liu M, Chen D, Xing YW, Spicer RA, Chen J, Them TR, Wang X, Li S, Guo C, Zhang G (2023) Mercury isotopes show vascular plants had colonized land extensively by the early Silurian. *Science Advances* **9**, 1–10.